Review

Razvan Stoian* and Jean-Philippe Colombier

Advances in ultrafast laser structuring of materials at the nanoscale

Abstract: Laser processing implies the generation of a material function defined by the shape and the size of the induced structures, being a collective effect of topography, morphology, and structural arrangement. A fundamental dimensional limit in laser processing is set by optical diffraction. Many material functions are yet defined at the micron scale, and laser microprocessing has become a mainstream development trend. Consequently, laser microscale applications have evolved significantly and developed into an industrial grade technology. New opportunities will nevertheless emerge from accessing the nanoscale. Advances in ultrafast laser processing technologies can enable unprecedented resolutions and processed feature sizes, with the prospect to bypass optical and thermal limits. We will review here the mechanisms of laser processing on extreme scales and the optical and material concepts allowing us to confine the energy beyond the optical limits. We will discuss direct focusing approaches, where the use of nonlinear and near-field effects has demonstrated strong capabilities for light confinement. We will argue that the control of material hydrodynamic response is the key to achieve ultimate resolution in laser processing. A specific structuring process couples both optical and material effects, the process of self-organization. We will discuss the newest results in surface and volume self-organization, indicating the dynamic interplay between light and matter evolution. Micron-sized and nanosized features can be combined into novel architectures and arrangements. We equally underline a new dimensional domain in processing accessible

now using laser radiation, the sub-100-nm feature size. Potential application fields will be indicated as the structuring sizes approach the effective mean free path of transport phenomena.

1 Introduction

The capacity of intense optical beams to modify and structure solids has been recognized almost at the same time with the invention of the laser [1], the first interactions with solid and soft matter being already reported in the beginning of the 60s [2–4]. Already before, optical means were employed in lithography to deliver small-scale structural features on solids [5]. Driven by a range of applications, laser ablation and material processing technologies strongly developed in the last decades [6] to approach smaller and smaller feature sizes down to the nanometer scale.

The interest in generating nanoscale feature sizes remotely using directional optical beams is tremendous. The reason is first related to a global tendency towards miniaturization, with compactness being a main drive in advanced processing. Secondly, and equally important, this is related to the fact that structuring a material generates a function. Resulting from topography or morphology landscapes and sizes, this function can be a consequence of scalability and packaging, e.g. a major drive factor in microelectronics, or it can be a genuine new characteristic of the solid, altering in a deterministic way its optical, contact, mechanical, and transport properties. The function being scale-dependent, it becomes thus of interest to structure solids on scales compatible with optical wavelengths for generating resonant optical responses or on scales comparable with collisional and ballistic processes to control energy transport and conversion. Local properties can thus be defined on mesoscopic scales to determine physical and chemical

*Corresponding author: Razvan Stoian, Laboratoire Hubert Curien, UMR 5516 CNRS, Université de Lyon, Université Jean Monnet, 42000 Saint Etienne, France, E-mail: razvan.stoian@univ-st-etienne.fr. https://orcid.org/0000-0003-2107-9515
Jean-Philippe Colombier, Laboratoire Hubert Curien, UMR 5516 CNRS, Université de Lyon, Université Jean Monnet, 42000 Saint Etienne, France, E-mail: jean.philippe.colombier@univ-st-etienne.fr

characteristics, for example, binding forces and specific surfaces in determining contact properties or in defining surface reactivity. The new function can be local, as the effect of single features with defined geometries, or nonlocal, depending therefore on a collective behavior of multiple nanoscale structures. Thus laser nanostructuring is more than just making nanoscale structures, it equally implies the understanding and the controlling of the process and of the function it generates.

1.1 Optical limits in laser processing: the challenge of confinement

The spatial scales of structures achievable with intense optical radiation are strongly related to the capability to focus light via optical systems [7, 8]. This represents a first necessary condition. A specific limitation originates from diffraction on finite apertures, with the concept of resolution being historically defined in the works of Abbe and Rayleigh. For a plane wave, one can define the optical limit as the diffraction limited spot diameter size $D = 1.22\lambda/NA$ or resolution $R = 0.61\lambda/NA$, with λ being the optical wavelength and NA the numerical aperture of the optical system. The limitation, both in the capacity of converging or collecting light, is intrinsic to finite apertures in far-field which filter high-frequency wavevectors. The dimensional down-shrinking effect for the irradiation scale can thus be enhanced by the use of smaller wavelengths and high numerical apertures and, for example, nowadays nanophotolithography techniques employ coherent UV or incoherent EUV light to generate nanoscale structures in the 10-nm range via the use of complex optical systems. A second necessary condition is to keep the energy within its optical limits, i.e. to arrest diffusive processes during the material evacuation. This can originate in the utilization of a shorter pulse duration, and present processing technologies increasingly employ ultrashort (10^{-15}–10^{-12} s) pulse laser sources.

The use of ultrashort optical sources has generated a paradigm in material processing. Fueled by advances in laser sources with significant upscale in power and frequency toward kilowatt class megahertz systems capable of high yields and driven by requirements of digital processing, the laser-based technology faces today the challenge of extreme resolution, granting access in a flexible and predictable way to the nanoscale The possibility to reach processing scales beyond the standard optical limits [9, 10] has pushed forward ultrafast laser processing techniques since their advent in the beginning of the nineties. Several concepts that will be outlined in the next sections were already tested at this point, namely the far-field and the near-field irradiation. Various ideas were explored including near-threshold interactions, nonlinear interactions, light-driven self-organization; all extrapolatable in two or three dimensions. A range of illustrative examples are given in Figure 1 that outlines several breakthrough developments in laser nanostructuring. They show results of employing direct focusing of intense light on glasses in the present of nonlinear excitation mechanisms induced by infrared ultrashort laser irradiation [11, 12] (Figure 1(a,b)), of using highly confined nondiffractive beams [13] for surface subwavelength structuring of transparent materials (Figure 1(c)) or of the employment of short-wavelength ultraviolet (UV) ultrashort laser pulses [14] for nontransparent materials (Figure 1(d)), where recent extension toward coherent extreme ultraviolet (XUV) [15, 16] can be noted. Examples of processing in near-field approaches [17, 18] are indicated in Figure 1(e,f) using field-enhancement and field-assisted optical proximity or apertureless close contact methods. Tight irradiation near the melting threshold will induce stress-driven hydrodynamic nanojets as shown in Figure 1(g) [19]. Parallel irradiation techniques can significantly increase the nanostructures production yield by taking advantage of multibeam interference or colloidal lithography [20, 21] (Figure 1(h,i)), and thus large areas structured at the nanoscale become viable concepts for exploring new functionalities. Light-driven self-organization effects, singular phenomena that couple coherently light and matter, are illustrated in Figure 1(j–m), showing the transition from subwavelength periodic patterns to high-resolution regular patterns and then to multiscale relief and nanoscale roughness [22–26]. These functionalities are not limited to surfaces but they extend into the bulk, designing nanoscale arrangements in three dimensions [13, 27–31]. Representative examples are given in Figure 1(n–s). These illustrate the concept of self-organization in the bulk [27, 28], void generation [13, 29], additive manufacturing [30], generation of nanoparticles via laser ablation [31], or, extending these concepts to soft and biological matter, nanosurgery and cell transfection [32, 33]. All these illustrate a large range of structural manifestations on the nanoscale triggered by light and show that extreme scales can be achieved, exceeding the commonly assumed optical limits. We will refer below to a generic dimensional scale, considered as a milestone in laser processing, the 100-nm scale, seen not necessarily as the absolute value but as a range of feature sizes much smaller that the generating laser wavelength, or comparable to its elevated harmonics. Beyond its performance comparable to a 10th of the wavelength, it appears as an enabling value for a radically different definition of the structured material.
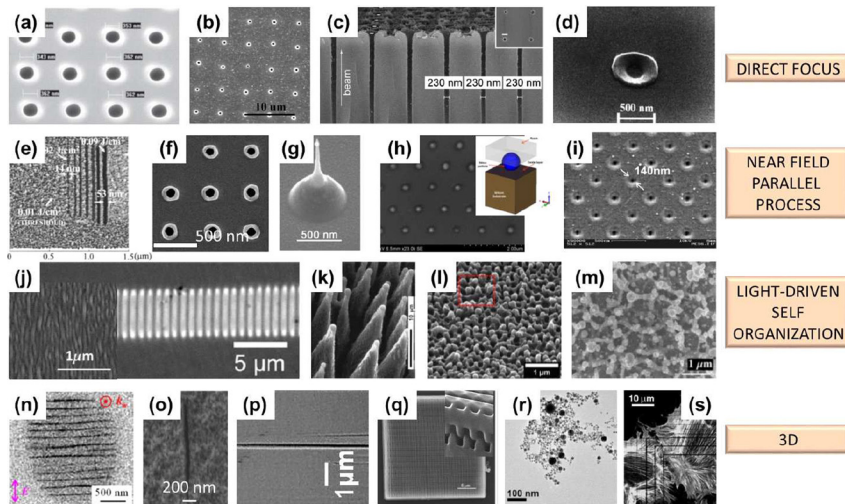
Figure 1: Example of ultrafast laser nanostructuring.
(a) Direct focusing and structuring beyond diffraction limit on dielectric surfaces. Reprinted with permission from a study by Joglekar et al. [11] ©(2004) National Academy of Sciences, U.S.A. (b) Nonlinear processing of glasses. Reprinted with permission from a study by White et al. [12] ©The Optical Society. (c) High aspect nanoscale structures on glass surfaces. Reprinted with permission from a study by Bhuyan et al. [13] ©American Institute of Physics. (d) Surface nanostructuring of semiconductors with UV ultrashort laser pulses. Reprinted with permission from a study by Simon and Ihlemann [14] ©Springer-Nature. (e) Field-enhancement–assisted nanoscribing of surfaces. Reprinted with permission from a study by Chimmalgi et al. [17] ©American Institute of Physics. (f) Apertureless near-field structuring. Reprinted with permission from a study by Kulchin et al. [18] ©The Optical Society. (g) Nanojets on surfaces. Reprinted with permission from a study by Ivanov et al. [19] ©Springer-Nature. (h) Parallel colloidal lithography. Reprinted with permission from a study by Khan et al. [20] ©Elsevier. (i) Parallel UV nanostructuring of surfaces. Reprinted with permission from a study by Klein-Wiele and Simon [21] ©The Optical Society. (j) Self-organization of subwavelength periodic surface structures under ultrashort laser irradiation. Reprinted with permission from a study by Garcia-Lechuga et al. [22] ©American Chemical Society. Inset. Self-organization on 100-nm scale. Reprinted with permission from a study by Nathala et al. [23] ©The Optical Society. (k) Laser-induced microcones relief. Reprinted with permission from a study by Her et al. [24]. ©American Institute of Physics. (l) Laser-induced nanocones landscape. Reprinted with permission from a study by Papadopoulos et al. [25]. ©Wiley. (m) Nanoscale roughness on surfaces. Reprinted with permission from a study by Vorobyev and Guo [26] ©The Optical Society. (n) 3D nanoscale light-driven self-organization in bulk silica glass. Reprinted with permission from a study by Shimotsuma et al. [27] ©American Physical Society. (o) Extreme nanostructuring in porous glass materials. Reprinted with permission from a study by Liao et al. [28] ©Royal Society of Chemistry. (p) Nanoscale structuring of volume glasses using nondiffractive beams [29]. (q) Three-dimensional additive nanofabrication using laser photopolymerization. Reprinted with permission from a study by Malinauskas et al. [30] ©Elsevier. (r) Laser-fabricated nanoparticles by ablation in liquids. Reprinted from a study by Doñate-Buendía et al. [31]. ©The Optical Society. (s) Nanosurgery in fibroblast. Reprinted from a study by Shen et al. [32] ©Tech Science Press.

1.2 The 100-nm cornerstone

The capacity of reaching super-resolution in laser material processing with access to sub-100 nm in a repeatable and reliable way is thus a major thrust of future developments and will lay the ground for the next generation of flexible and precise material processing tools. From the perspective of processing performance with a remote optical beam, the 100-nm scale represents a cornerstone, where the processed functions depend not only on local (mesoscopic) topographies but also on the onset of collective effects. This is of interest in transport phenomena in solids, where the mean free path in collisional transport by electrons and phonons becomes comparable with the feature size, laying down the possibility to control energy exchange and fostering advances in mechanics and energy, notably mechanical and thermal management, in chemistry, with locally engineering chemical properties, as well as in optical processes, sampling wavelengths and optical signals for information technologies. Thus advanced beam management and control mechanisms are being applied to achieve extreme spatial scales with optical means, some of them being explored in the next sections.

Making a review of all the effort invested so far in laser nanostructuring is most certainly a too ambitious task and definitely a challenge. Observing the recent advances, this works aims at exploring general ways of generating extreme processing scales using optical radiation that can be truly assigned to nanotechnologies. It will revisit main concepts to achieve super-resolution in ultrafast laser

processing and it will intuitively illustrate how to overcome optical limits. It will discuss several mechanisms relying on direct focusing, focus engineering, and light-driven self-organization, harnessing the nonlinearities provided by the intense short beams. All these concepts apply for surfaces and to the bulk, and are relevant for a range of materials in two and three dimensions, an essential characteristic of remote optical processing beams with respect to present alternatives. The latter define the economical impact of the laser technology. We will then indicate the main functions related to a nanoscale topography that will define optical, mechanical, chemical, or contact properties. But mostly, this review aims at being a plea for efficient use of photons to structure materials beyond the standard accessible optical scales.

2 Direct focusing on the nanoscale

The most forward way to structure a solid is to direct an energetic optical beam on its surface with enough intensity to excite and ablate the material. Most of the beam profiles focused through an optical system and subject to diffraction can have their projections in far-field on a surface approximated by an Airy or Gauss spatial profile of the focal spot. This is spatially defined by its waist diameter limited by diffraction to a finite minimal value, as depicted in Figure 2(a). Most performant optical systems provide a far-field spot limited by diffraction on the scale of approximately half of the optical wavelength, roughly 200–500 nm for the visible and near-infrared spectral range. However, irradiation in specific energy conditions creates impact spots well below this value. Examples of irradiation fingerprints are illustrated in Figure 2(b–d)

where structures as small as 50 nm can be obtained. Obviously, these values are much smaller than the beam size for reasons that will be discussed below. We stress that, in defining accuracy and resolution in the present context, we consider mainly radial dimensions. In specific cases, the axial dimension and the protrusion depth can equally be of interest.

2.1 Threshold interactions

Firstly, the ablation scale depends on the extent of energy concentration. A prime condition is that this does not exceed the initial energy deposition area. Diffusive mechanisms, notably heat transport may enlarge the domain, with potential to generate physical ablation effects outside of the optical area. Illustrated in Figure 3(a) (the figure shows the extent of optical and diffusing energy) this implies that the diffusion length should be small. Considering a simple case of heat transport, L_{diff} is on the order of $2\sqrt{D \cdot \tau_{\mathrm{thermal}}}$, D being the diffusivity and τ_{thermal} the process time. This condition imposes a small time of the process. In laser processing, the relevant process time is considered to be the time required to heat the matrix [35], making the use of short pulse ubiquitous. This represents an approximative but generic description of a characteristic diffusion length [35, 36], depending on assumptions on the initial boundary conditions particularly when the spot and process times become small, and on the type of relevant transport mechanism (electrons, phonons). Furthermore, the consideration of ablation will require the utilization of numerical models. The use of ultrashort laser pulses puts forward the following points to consider. To have a relevant and efficient process capable of producing
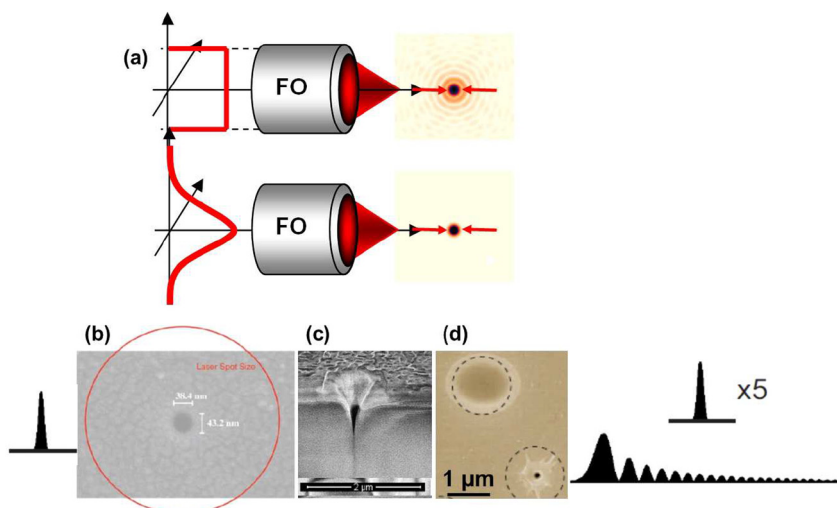
Figure 2: (a) Focusing a beam through an optical system. (b) Near-threshold focusing on a glass substrate. At the tip of the Gaussian beam profile, structures smaller than the waist are obtained. Reprinted with permission from a study by Joglekar et al. [11] ©(2004) National Academy of Sciences, U.S.A. (c) Nolinear focusing with aberration-engineered beams. Reprinted with permission from a study of White et al. [12] ©The Optical Society. (d) Nonlinear focusing with time-engineered beams. Reprinted with permission from a study by Englert et al. [34] ©The Optical Society.
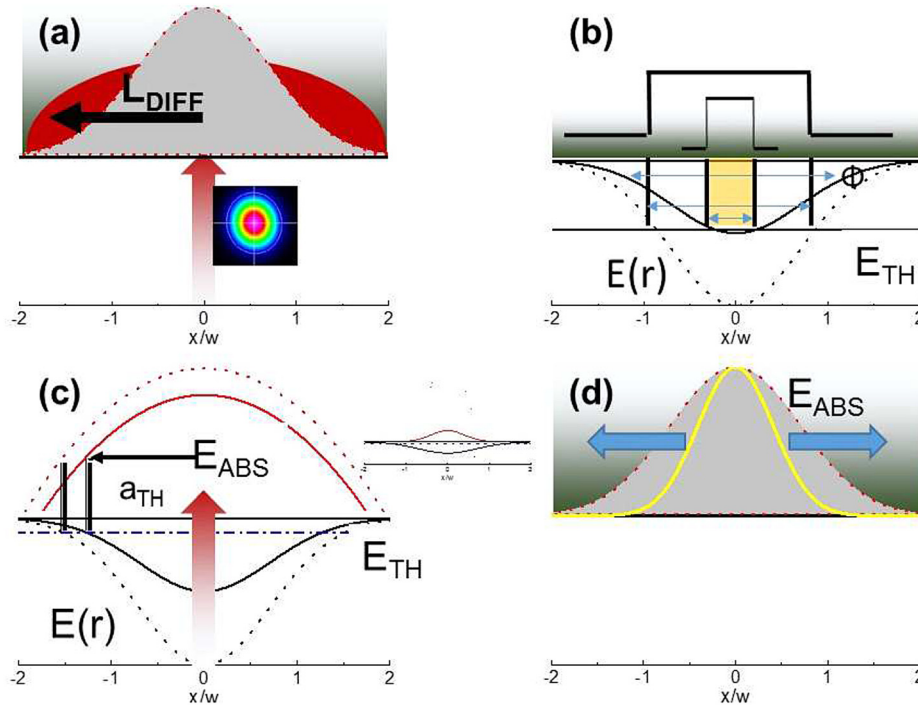
Figure 3: (a) Competition between optical limits and energy diffusion. Energy diffuses thermally outside of the optical concentration area on a range given by the diffusion length L_{DIFF}. It is to be noted that the spread of energy can give ablative effects if the energy concentration stays roughly above the vaporization threshold or structural material modifications below this value. (b) Threshold filtering of ablative areas. The extent of ablative region (Φ) is indicated for two fluence values. A narrow region is found for near-threshold irradiation (E_{TH}). (c) Nonlinear effects on processed areas. A linear distribution of input energy $E(r)$ is given on the surface for two fluence values, and corresponding nonlinear absorption profiles E_{ABS} (assumed three photon absorption) are given beneath the surface (logarithmic scale). The ablated crater edges depend only on the linear energy distribution profile. (d) Material response in the excited areas. A fast hydrodynamic material response occurring at the speed of sound under constraints will be limited to the nanoscale, having a narrower profile than the original excitation.

a physical modification effect, $\tau_{thermal}$ can be given by the time needed to build the heat source, allowing us to diffuse away the energy beyond a threshold causing material removal or modification. For very short pulses, $\tau_{thermal}$ is defined by electron-phonon coupling (few ps) and indicates the limit in the diffusion length L_{diff} which ranges on a scale comprised between few nanometers and few tens of nanometer (and more if the source is repetitive and the regime cumulative). If diffusion continues naturally beyond this time, cooling will make the process less relevant for permanent material modification effects. The overall diffusion and evolution of the energy flux will be precisely defined by the geometry, localization, and by the temporal form of the thermal source delimited by the photoexcited regions. Most important is that, for ultrashort pulses, the energy deposition rate is high, triggering fast heating and therefore fast material removal almost on the same scale. The energy will be carried away by ablation products, leaving less heat deposit, and no significant diffusion occurs beyond the optical spot [37].

Secondly, the beam waist is a convention quantity characterizing a spatial distribution of photons (peak spatial energy concentration induced by a wavefront curvature measured at $1/e^2$) while an ablation footprint is the effect of a physical process, i.e., whenever the energy outpaces the ablation threshold, a structure originating from material removal is formed. From here, the second criterion of super-resolution is achieved, namely working at energy inputs where the threshold is surpassed on a narrower region of the Gaussian. The process is illustrated in Figure 3(b) for two fluence values, showing the forecasted size of modification for each fluence value. The existence of an energy threshold of the ablation process (shown by the horizontal line) limits the material removal to the only region where the input energy exceeds this threshold. Accurate control of energy just above the threshold creates a limitation of energy deposition area which becomes smaller than the optical beam dimension. This represents a major conceptual advance for laser nanostructuring and depends essentially on a property of

ultrashort pulse irradiation; its deterministic character. Deterministic interaction with light implies here that in various materials, notably in dielectrics, the optically intense radiation generates its own absorption centers and does not rely on extrinsic, statistically distributed factors to deposit energy (e.g., impurities and pre-existing structural defects), minimizing thus fluctuations in energy deposition [11]. The irradiation becomes stable with respect to the threshold. This is eventually more pronounced for wide bandgap materials where several photons absorbed instantaneously are required to bridge the energy gap, initiating further absorption on thus-generated free carriers, but equally applies for linear materials where fluctuations-free absorption is granted by a well-defined band structure all along the processed area. In principle, the feature sizes can become indeed very small; however, accurate control is required for the smallest intensities due to the flattened top of the Gaussian energy distribution. Joglekar et al. [11] used precise control of the beam energy with respect to a deterministic material ablation threshold and created the conditions that just the tip of the Gaussian distribution exceeds the threshold. Ablation occurs in the restricted zone over the threshold. Thus they demonstrated a remarkable below 100 nm nanomorphing capacity.

The thresholding concept was equally applied not only for ablative processes but also in the melting domain, where stress and liquefaction will generate nanoscale hydrodynamic phenomena in the form of nanojets [38]. These kinds of processes are now the object of advanced simulation techniques including molecular dynamics [19] and continuum elasto-plastic models [39]. Hydrodynamic expulsion with threshold control is now established in laser-induced forward transfer to remote print nanoscale droplets or material parts [40], or, as well, in the production of nanoparticles [41]. These were the object of several reviews [42, 43] and will not be discussed here.

2.2 Nonlinearity of laser interaction

A second element is related to a potential nonlinearity of interaction. Let us take, for example, the case of a dielectric material, where the high intensity of the focused ultrashort beam ensures sufficient density of photons to bridge nonlinearly the electrons over the gap (metals can equally show nonlinear carrier heating to upper band levels). The nonlinear character of absorption (e.g. multiphoton absorption) suggests intuitively that the material sees a spatially varying beam profile as a power function of the incident beam profile $I(r)$ and becomes thus narrower. Similarly, the intensity has a time-varying behavior,

enhancing the nonlinearity. Assuming an N photon ionization process, the absorption profile matches approximately $I^N(r, t)$, reflecting a transition probability nonlinearly proportional to the photon density. The absorption profile becomes narrower. This pertains particularly to Gaussian spatial distributions of the electric field $\mathcal{E}(r) = \mathcal{E}_0 \exp(-r^2/w^2)$. The nonlinear character was advocated for developing high-aspect nanostructures in glass by White et al. [12]. The question is now, how essential the nonlinearity can be in determining small ablation spots? Recently, Garcia-Lechuga et al. [44] argued that, given the fact that the threshold is deterministically related to a specific amount of input energy, the processing size should be independent of the nonlinearity of interaction. A characteristic situation is described in Figure 3(c), where the linear distribution of input energy is given on the surface and a nonlinear absorption profile is given beneath (logarithmic scale for an assumed three photon process). This represents thus the exposure part and the absorbed part (the inset shows the linear representation). Despite the fact that it is the absorbed energy that creates the physical effect, the threshold quantity is defined by the incoming energy distribution. It appears indeed that, irrespective of the nonlinearity, the ablative crater is only given by the linear distribution of energy with respect to the threshold value. The latter is defined by material and by the irradiation conditions (wavelength, pulse duration), creating different processing sizes for various materials and pulse durations, but still defined by the initial distribution of input energy. A relative constancy of the spot relative to the threshold was found [44]. However a point should be made here. If the edges of the affected area are set by the linear profile of the incoming beam, the absorption profile will create nevertheless a narrowing of energy deposition. In conditions of strong focusing and in the presence of various physical thresholds of material modification and ablation, the depth profile of the modification becomes such that a narrow size can be claimed. Also, given the strength of material removal, several thresholds can be defined, and observations of gentle and strong phases were made relatively early [45]. Englert et al. [34] have demonstrated that the use of asymmetric pulse profiles regulating multiple nonlinearities (i.e. multiphoton and collisional multiplication) can induce in similar focusing conditions much narrower and deeper structures as compared to Fourier transform pulses, a situation illustrated in Figure 2(d).

If the role of nonlinearity on surfaces is a matter of debate, for volume nanostructuring it becomes a key element. Notwithstanding propagation elements that will be recalled in the next section, the excitation profile in transparent materials becomes a nonlinear function of the incident intensity distribution, at least for low

exposure rates. This translates into a similar profile of ionization-induced broken bonds. In combination with chemical methods to expose the laser-affected volumes, Ródenas et al. [46] demonstrated a high capacity of fs laser nanolithography of bulk optical crystals. Volume direct nanostructuring requires a good regulation of light delocalization factors via the focusing strength and the energy level in order to harvest the benefits of nonlinear ionization for volume nanostructuring.

## 2.3 Material hydrodynamics: a nanoscale response

The presence of a narrow absorption profile indicates also an alternative processing route to reach scales almost independently of the optical size. Under strong excitation gradients giving specific relaxation patterns for pressure and temperature, a thermomechanical material response occurs in the form of heating, hydrodynamic movement, material failure, rupture or cavitation [47] if the elastic limited is bypassed. These phenomena are dynamically limited by the speed of sound c_s and, for relaxation times in the tens of ps range, the spatial extent $d = c_s \cdot \tau_{\text{relax}}$ is on the nanoscale. The characteristic time corresponds to processes ranging from ballistic transport to shock release and rarefaction, depending both on the size and the amount of energy concentration. The situation is illustrated in Figure 3(d), where a narrower structuring profile can be established for a given excitation. The concept of nanocavitation with the formation of nanobubbles and movement of interfaces was proposed for interaction with soft and biological materials [48]. It is therefore important to note here that super-resolved laser processing can be obtained without the actual need to bypass a diffraction limit as it does not explicitly rely on an optical effect. The approach represents thus a change of paradigm. This being said, an indirect relation persists as the size of the source defines in particular cases the gradients of constraints and the diffusion area. Harvesting all the potential of the technique requires nevertheless control over the interaction processes and the speed of energy transport, and thus notably over the achieved nonequilibrium among all its forms; electronic nonequilibrium, structural nonequilibriums, thermodynamic and mechanical nonequilibrium. Access to various forms of nonequilibrium is quintessential, where electronic nonequilibrium defines the very first steps of energy transport, the structural nonequilibrium being a channel of energy consumption, and the thermomechanical nonequilibrium the drive force

behind material rupture. All these forms require advanced methods of observation and control that will be described latter in the text.

2.4 Focal engineering and near-field processing: sub-wavelength light localization

An extrapolation of direct focusing approaches for obtaining higher resolution relies on optical engineering, illustrated by several examples in Figure 4. Already superlens concepts are being applied in lithography or imaging based on photonic crystal and metamaterial design [49] aiming to achieve resonances [50] or negative refraction [51] and perfect focusing. This focusing feature derives from a capacity of exploiting high-frequency evanescent wavevectors in phase and amplitude. Current superlens approaches propose a combination of near-field and far-field effects that renders a facility of exploitation and resolutions of few tens of nm [52]. An example is given in Figure 4(a) [52]. If their design is complex and their employment is a trade-off between working distance and accessibility, they represent a potential path for achieving super-resolution in laser material processing, alongside of other optical engineering techniques inspired from super-resolution microscopy [53].

The concept of diffraction limit is defined by the apparatus-imposed filtering of high-frequency wavevectors. Near-field approaches [59] allow us to access the evanescent fields and to achieve a stronger concentration of light. Several methods rely on the field-enhancement capacity of narrow physical probes irradiated by laser radiation in the proximity of the surface, combining light near-field confinement and ultrashort nondissipative energy fields to ablated matter [60]. An example is given in Figure 4(b) showing a capability of structuring of few tens of nm [54, 55]. Similarly, optical probes, particles or microspheres in optical proximity can create light concentrations and ablative effects on the nanoscale 61–65. This is illustrated in Figure 4(c) employing self-organized arrays of microspheres [56]. Light concentration by a dielectric sphere and far-field acquisition has been proposed to achieve resolutions in microscopy exceeding $\lambda/5$ using far-field projection of near-field images [66]. Upon focusing, light is concentrated in a subdiffraction-limit progressive beam known as photonic jet [67], and the technique was applied in laser processing for approximately two decades [61, 62, 68]. A further characteristic should be retained here. With respect to other near-field techniques based on field-enhancement around probes, the colloidal patterning is a parallel, high-yield,
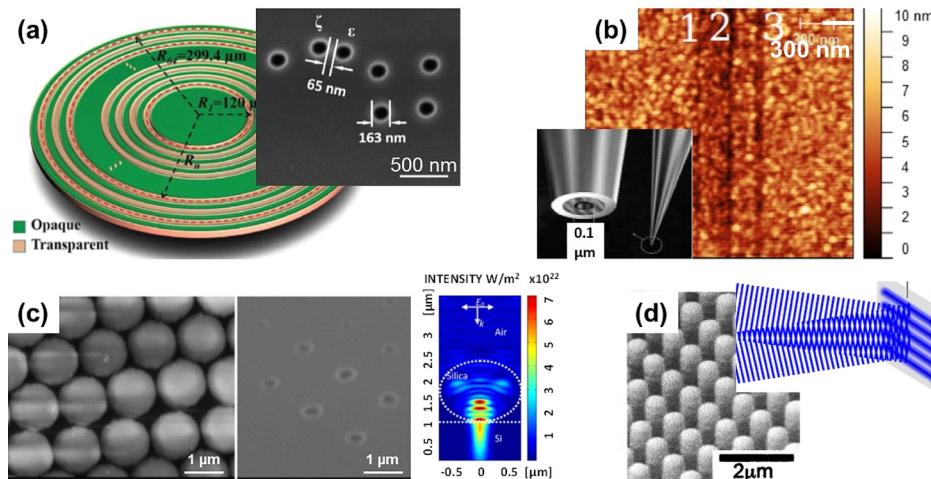
Figure 4: (a) Type of super-lens design for imaging beyond diffraction limit. Reprinted with permission from a study by Qin et al. [52] ©Wiley. Example of probe-assisted field enhancement for nanoscribing. Reprinted with permission from a study by Falcón Casas and Kautek [54] ©MDPI. Insert: near-field probe types. Reprinted with permission from a study by Korte et al. [55] ©Elsevier. (c) Colloidal laser-supported lithography using arrays of microspheres. Insert: Light focusing by microsphere. Reprinted with permission from a study by Sedao et al. [56] ©Springer. (d) Parallel processing by multibeam interference. Reprinted with permission from a study by Kondo et al. [57] ©American Institute of Physics. Insert: Conceptual description. Reprinted with permission from a study by Burrow and Gaylord [58] ©MDPI.

high-throughput technique. If here the parallel effect comes from the self-assembly (colloidal behavior of microspheres) of single lenses creating a multitude of singular focusing points, a similar effect derives from the interference of multiple beams and the imprinting of complex light patterns [21, 58]. The latter is illustrated in Figure 4(d) combining short wavelengths and ultrashort durations. Super-resolution below 100 nm was demonstrated with pattern features in the 20-nm range [69]. Employing multiple beams, the concept carries a three-dimensional character, being utilized for example for additive manufacturing by multi-photon polymerization [57].

Triggering near-field effects is not limited to external probes of focusing elements, artifacts on the material surfaces can act as nanoscale field enhancers. This is the case of singular topography features on surfaces (holes or bumps) which can scatter light and lead to localized field enhancement. Recently, these enhancers were used to seed nanoscale field confinement in a direct writing scheme, leading to a writing strategy capable of developing nanoscale patterns with feature size in the 20 nm range, using polarization and scan parameters as control knobs [70].

3 Self-organization on surfaces: order in a nanoscale topography

We have argued above that a straightforward way to structure a solid is to direct an energetic beam towards the surface that will ablate the material. Besides direct

ablative processes, another type of structuring phenomena occurs on excited surfaces, a topography transformation into a periodic pattern with sub-wavelength periodicities, the laser-induced periodic surface structures (LIPSS) [71]. Recently reviewed in a study by Bonse and Gräf [72], the question of the formation of anisotropic regular structures on materials irradiated by light fields of isotropic and uniform energy distribution is a key issue in controlling laser structuring processes below the diffractive limit.

Observed first by Birnbaum [73] on semiconductor surfaces, these periodic structures have suscitated a large interest, being identified on practically all classes of solid materials [74] and for a large range of irradiation parameters, including ultrashort laser pulses. Often related to a polarization state, these structures respond to a vectorial anisotropy of the beam [71]. This particularity supported formation scenarios based on light scattering and interference processes driven by incoming and scattered waves with evanescent components in the vicinity of the surface [75], forming a standing pattern. Radiative and nonradiative components concur to define spatial orientations and periods. The Sipe theory [75], a radical advance in the field based on a scattering formalism, defines an optimal field spatial pattern which is driven by topography, with a figure of merit called efficacy. These approaches were complemented with electronic excitation models, permitting to vary in real time the optical properties of a solid as a function of the quantity of excitation, primarily used for bandgap materials in the presence of laser-induced free carriers [76].

In parallel material scenarios were considered, where destabilized surfaces can reorganize along specific proper modes [77, 78], based on pattern similarities with ion sputtering [79]. Here empirical dynamic reorganization models based on Kuramoto-Sivashinsky formalism [77, 80] were suggested to emulate laser and ion-triggered arrangements in forms similar to Turing patterns [81]. In either perspective, intrinsic self-organization or light-driven, the topography implies matter displacement [82], where also specific spatial frequencies are allowed by a potentially involved melt pool [83].

The two scenarios are reconciled with the concept of feedback where light motifs push matter to follow, exercising in turn an effect on the upcoming optical patterns, a nonequilibrium entropic evolution of the light-matter ensemble. The dissipation of energy becomes organized. A nonlinear feedback mechanism, ubiquitous in dynamical systems, was identified, carrying positive and negative feedback components driving and respectively stabilizing the growth and the ordering of structures [84]. The photo-excited region evolves far from equilibrium with fluctuations coming from near-field enhancement on local surface relief. Such fluctuations are crucial to set off inhomogeneous thermal gradients driven by energy absorption and potentially triggering instabilities. The system gains complexity and a nonlinear and adaptive behavior is reached as a steady state upon multipulse excitation. According to Prigogine [85], through positive feedback amplifying any disturbance in the system, a bifurcation point arises that forces the system to reorganize into dissipative structures forming a coherent state. Apparent negative entropy production of the arranged surface on the mesoscale is balanced by irreversible microscopic processes such as structural modifications and defects or even entropy production by light scattering during the process [86]. The feedback is active on two levels, a topography driven effect acting pulse by pulse and a transient effect of spatially selective optical properties during the exposure. Accurate control of feedback results then in the generation of highly regular structures and patterns where light and matter mobility and flow are synergetically synchronized [87, 88]. The latter acquires a significant importance in the order quality of the structures. High level of order was observed, for example, on bulk metallic glasses, where potentially the particular flow characteristics of amorphous metals play a major role [88].

Within the electromagnetic scenario, the surface waves participating in establishing a standing pattern in interaction with the incoming light are often identified with the surface plasmon polaritons [89], coupling light and material. Recent advances proposed tuning of the optical properties of interfaces to allow for plasmonic processing [90]. Taking into account that particular optical conditions should apply to support plasmonic propagation in view of its dispersive behavior and the necessity to conserve momentum and energy, plasmonic waves were often considered to be the dominant contribution in the scattered surface wave. Notwithstanding the conservation laws, plasmonic resonances depend on the relief topographies and on the corrugation depth, with the spectral signature evolving. We indicate nevertheless that it is eventually the overall evanescent field distribution emerging from the interference of scattered waves and incident waves that will define LIPSS periodicities. It is to be noted that various
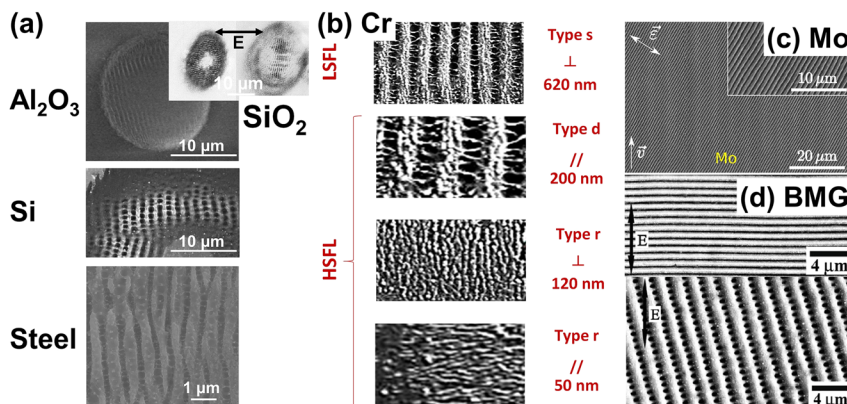

Figure 5: (a) Top: Regular ripples on dielectrics. A sapphire (corundum) surface irradiated with multipulse ps laser radiation slightly above the ablation threshold is shown. Inset: examples of parallel and perpendicular close-to-wavelength ripples on fused silica upon irradiation with few 200 fs pulses at two different fluence regimes, low (left) and high (right). Middle: Ripples on silicon. Bottom: Ripples on stainless steel. (b) Multitude of periodicities and orientations observed on chromium, classifying the types of currently observed laser-induced periodic surface structures (LIPSS) [92]. (c) High order arrangement on molybdenum. Reprinted with permission from a study by Gnilitskyi et al. [87] ©Springer-Nature. (d) Regular structures on bulk metallic glasses. Reprinted with permission from a study by Zhang et al. [88] ©Springer.

LIPSS classes were observed aligning parallel or perpendicular to the field direction as a function of the local dielectric function, and ranges of periodicities similar to harmonics of the main arrangements were put into evidence. An example is given in Figure 5, showing typical types of close-to-wavelength and subwavelength ripples on dielectrics, semiconductors, and metals. Figure 5(a) identifies types of low-spatial frequency ripples on dielectrics (sapphire, fused silica) with various orientations with respect to polarization, on silicon, and on stainless steel. In a scattering model, the orientation is simply set by the scattering pattern around rugosity features, parallel to the field for dielectric optical properties and perpendicular to the field for metal-like optical properties [71, 91]. Figure 5(b) shows the type of periodicity scaling obtained by tuning irradiation conditions, down to high-frequency spatial structures (HSFLs). We retain that sub-100-nm structures and periodicities can be obtained. The reason for the extreme values lies in the evanescent character of the field pattern.

Recent advances in the comprehension of LIPSS were made using a combination of interrelated electromagnetic and material models [93, 94] coupling self-consistently electromagnetic and hydrodynamic approaches. The ansatz implies coherent scattering on surface roughness that can be intrinsically produced by laser radiation [75]. The idea implies two main points. The interference relies on a generalized concept of surface waves that do not necessarily depend on plasmons, different types of evanescent waves [95–97], for example, the so called quasi-cylindrical waves, being present, and, in view of less restrictive conditions for their excitation, potentially widespread. Nonlocal far-field and local near-field contributions can be identified in the patterns, their weight being dependent on the superficial concentration of scattering centers [98]. The second point is related to the origin of roughness. As the surface relaxes quasi-one-dimensionally by emitting pressure waves into the bulk, being in return subject to rarefaction, local cavitation will determine material failures and will form cavities creating further field enhancement and scattering of incoming radiation [99]. In addition, fast cooling and quenching determine structurally defected regions [100], contributing to the complex field response. The scenario is graphically represented in Figure 6 showing wave and material contributions. The coherent scattering imprints patterns close to the wavelength, made mostly by nonlocal far-field contributions (Figure 6(a)). Cavitation-driven formation of scattering centers is enhancing the coupling to the incoming light (Figure 6(b)), forming topographical arrangements and structural disordering (inset Figure 6(b) [99, 100], note the regular nanocavities appearing under the surface and the concentration of defects). Multipulse feedback will increase order and will stabilize the period slightly below the fundamental wavelength (Figure 6(c)). Local near-field contributions determine higher frequency patterns. The extreme scales and the stablization of periodicity follow nevertheless a different, nonstandard scenario. Local hydrodynamic instabilities and thermal flow driven by radiation self-arrange into patterns with feature scale going
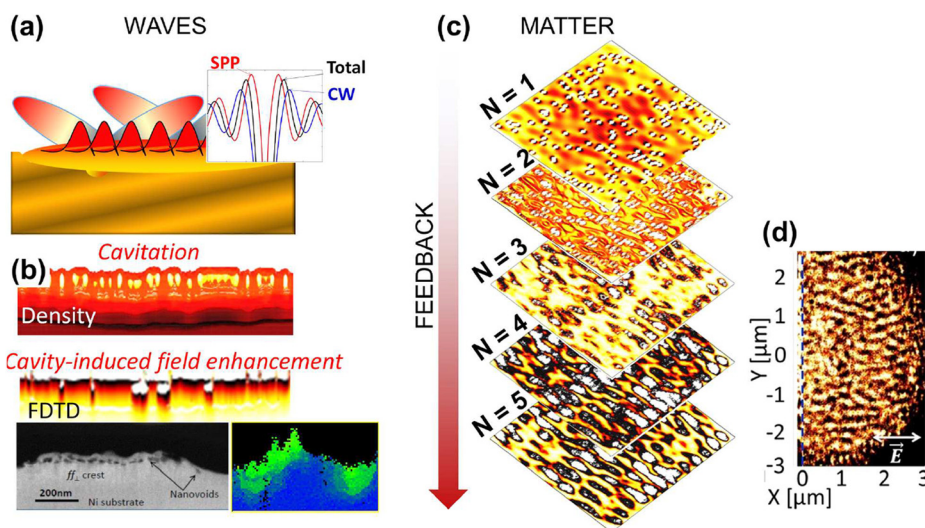
Figure 6: Laser-induced periodic surface structure (LIPSS) generation steps based on light and matter contributions.
(a) Schematic of light scattering, of the emergence of surface waves, and of standing patterns, with examples of surface plasmon-polariton (SPP) waves and cylindrical waves (CW). (b) Rarefaction-induced cavitation and field enhancement. The inset shows measurements of nanocavities (by transmission electron microscopy) [99] and structurally defected regions (concentration of defects measured by electron backscatter diffraction) [100]. (c) Gradual formation of ripples under multipulse excitation, with the emergence of a regulating feedback.
(d) Small-scale self-arrangement driven by hydrodynamic instabilities on the surface.
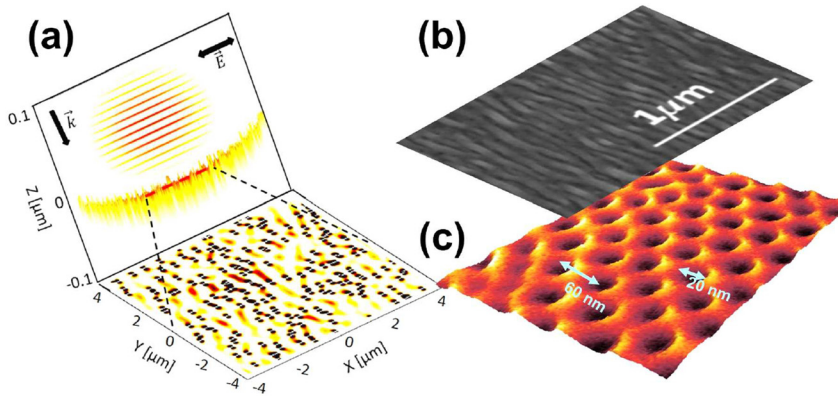
Figure 7: (a) Conceptual illustration of light and material patterns. (b) High-frequency spatial structures (HSFL) with sub-100-nm periodicities. Reprinted with permission from a study by Nathala et al. [23] ©Springer-Nature. (c) Nanohole pattern on single crystal surfaces irradiated with double pulse sequences with polarization control [101].

beyond $\lambda/10$ (Figure 6(d)); the sub-100-nm range being thus attainable. This demonstrates a synergy between evanescent field confinement and a nanoscale material response i.e., the formation of cavities.

The formation of particular landscapes is connected to scattering patterns. The denser the scattering sites are the denser the light patterns will be. This first implies that control of light distribution will enable the achievement of extreme scales. Figure 7 depicts several particular achievements based on scattering control (conceptually illustrated in Figure 7(a)), with dense 100 nm HSFL (shown in Figure 7 (b)) [23]. Pushing more the coupling between radiation and landscape, further record sizes can be demonstrated. Abou-Saleh et al. [101] have indicated using double pulse sequences the emergence of other types of 2D high-resolution patterns (notably hexagonal), where the regulation concept comes from combining crossed-polarization and time-delay for irradiations close to the modification threshold. This particular parameter range promotes geometry complexity and, notably, structural size well below 100 nm. This achievement relates intimately to the state of the surface. On softly excited surface in evolution, transient instabilities will create dense nanoscaled landscapes that will couple light (particularly nonradiative fields) and determine a dynamic system relaxing in a form of a Turing-like pattern. Diffusive and convective heat transport and the associated hydrodynamic movement in a destabilized liquid layer will define, depending on the Marangoni number, extreme scales and novel periodic arrangements as competition between vectorial light character and hydrothermal waves [94]. This situation is illustrated numerically in Figure 6(d) and experimentally in Figure 7(c). It is then important to note that several factors may concur to the achievement of very small features; a high density of scattering centers favoring near-field interaction, strong field confinement, and transport coefficients that will limit the diffusion of energy, washing out the gradients.

4 Nanostructuring in volume: from nanocavitation to 3D self-organization – a universal material response

All the above concepts apply not only for surface interactions, they equally apply for volume excitation of materials normally transparent to the incoming radiation wavelength. In this case the achieved intensity upon focusing excites the solid nonlinearly and generates absorption. However, differently from a surface impact, a bulk interaction implies transporting the laser radiation at the impact point inside the volume. This includes linear and nonlinear aspects of light propagation including dispersion, self-focusing, self-phase modulation and many other effects that change the pulse envelope, its phase, or the arrival order of frequencies. The peak intensity becomes a key element, being defined by counteracting phenomena; focusing and self-focusing tending to increase the intensity beyond a catastrophic threshold, while diffraction and scattering on mobile and light carriers having the inverse effect. From the material side, additional constraints appear on matter transport due to spatial confinement. These aspects were reviewed several times [102, 103] and were recently revisited in [104] in the context of laser volume nanostructuring. Whenever the energy at the impact point overcomes the material resistance, a structuring phenomenon takes place. If the spatial dimension critically relies on nonlinear excitation, it will be finely defined by plasma relaxation, phase-transition, pressure release, and rarefaction.

The first concept relevant for bulk nanostructuring is the concept of microexplosion [105], implying fast excitation in high dense plasmas, development of multi MBar of electronic pressure, shock, and rarefaction. A cavity is formed, surrounded by denser regions, with a dimension

that reflects the energy concentration. Nanoscale structures were obtained by tight focusing of nJ ultrashort laser pulses [106], being equally the birthplace of new structural arrangements in the highly densified limits [107]. Two concepts were discussed recently; cavitation in the solid phase in materials with high Young modulus [106] driven by shock, or, in case of strongly coupled materials (e.g., fused silica with the characteristic exciton trapping due to strong interaction between electrons and matrix), cavitation from a rapidly formed liquid phase (that relaxes internal mechanical constraints) subject to stress [108]. In both cases, in view of a short relaxation time in the ps-ns range, the material opening at the speed of sound at most leads to structural sizes of void-like regions in the 50–200 nm range. Careful energy control can lead to even smaller structures. The concept is illustratively sketched in Figure 8(a) where the two situations are depicted. Each case shows as well its characteristic constraints fields, respectively pressure and stress driven. Figure 8(b–e) shows particular examples, with nanoscale void-like structures produced by fs and ps single pulses in hard corundum using Bessel (Figure 8(b,c)) and Gauss beams (Figure 8(d)), as well as void-like structures produced by ps Bessel beams in fused silica. One point of observation should be made here. As compared to soft, material-dependent excitation regimes at low intensities (which, combined to chemical methods to reveal structures, can also lead to nanostructuring [46]), the structuring process indicated here relies on a general plasma-mediated drive. If cavitation is the result of strong excitation, two channels compete to relax the absorbed energy; the mechanical

relaxation of the solid via shock and rarefaction and the material heating and phase transformation. The border between the two mechanisms can be tuned by choosing material-dependent pulse durations, and transition from cavitation to liquid and gas-phase nucleation seems to be driven by increasing pulse durations [109]. Irrespective of the specific dynamics, from a thermal point of view, the excited material is at the border between mechanical rarefaction and nucleated phase transitions to gas-phase and molecular decomposition [110] (witnessed, for example, by the signature of molecular oxygen in volume structures in oxides [111, 112]). This will be the birthplace of a self-organization phenomenon, discussed below.

The excitation in the volume is equally at the origin of the spectacular effect of 3D self-organization (Figure 1(n)), the formation of nanogratings and their polarization and birefringence function. Discovered by Shimotsuma et al. [27] in bulk fused silica, soon after the demonstration of bulk modification of soft and strong positive index regimes [105, 113], they manifest polarization-dependent order and periodicities on the $\lambda/2n$ scale, and relate to the behavior of localized plasmas in electric fields [114]. These were first indications describing the reshaping of nanoscale plasmas under strong fields and the development of potential resonances. Building up on electromagnetic scenarios coupled with transient excitation models, Buschlinger et al. [115] and Rudenko et al. [116] have developed models describing the periodic arrangement of carrier plasmas in the electric field. The main ansatz, as for LIPSS, is the process of scattering on pre-existing or on laser-induced scattering centers, initially random-distributed, and the
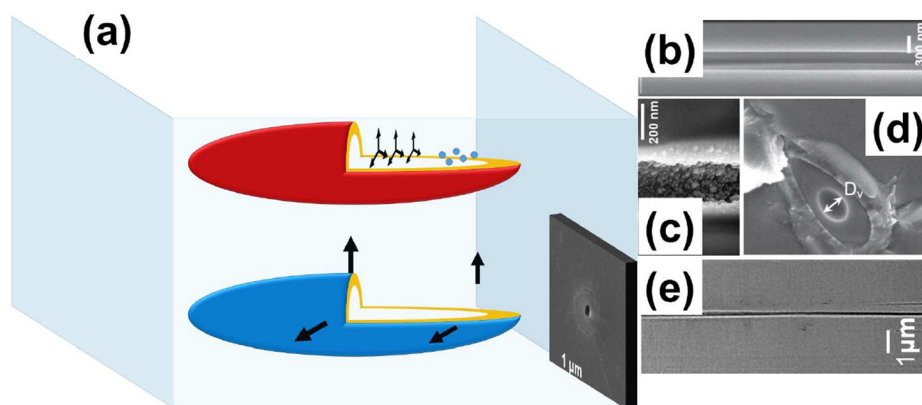
Figure 8: (a) Illustrative concepts for shock-driven cavitation in the solid phase and stress-driven cavitation in the liquid phase. (b) Fs-pulse induced cavity in sapphire with nondiffractive beams. Reprinted with permission from a study by Rapp et al. [109] ©Springer-Nature. (c) Ps-pulse induced cavity in sapphire with nondiffractive beams. Reprinted with permission from a study by Rapp et al. [109] ©Springer-Nature. (d) Fs-pulse induced cavity in sapphire with Gauss beams. Reprinted with permission from a study by Juodkazis et al. [106] ©American Physical Society. (e) Fs-pulse induced cavity in fused silica with nondiffractive beams [29].
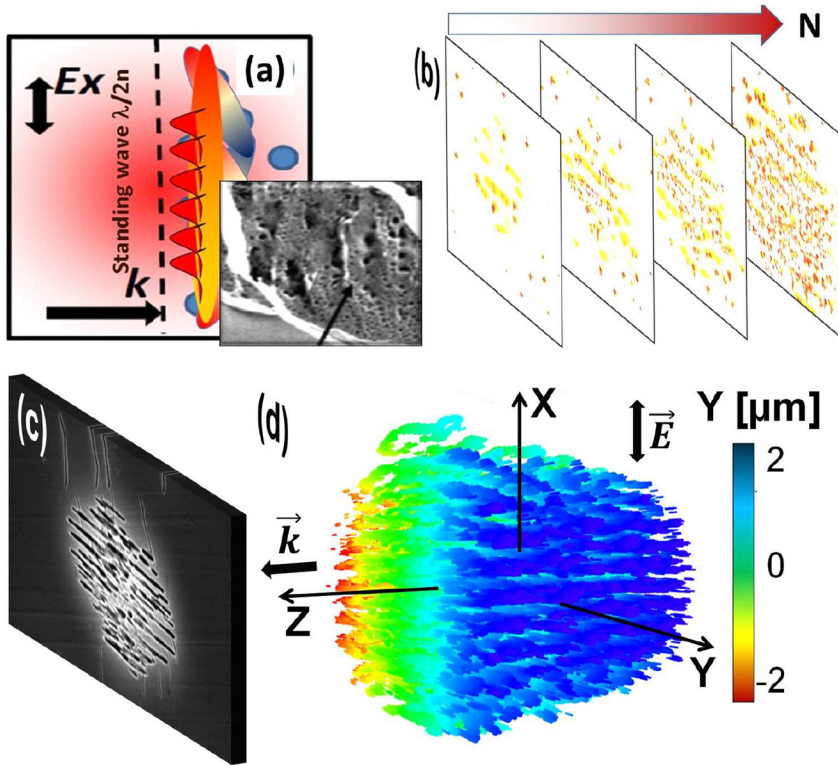
Figure 9: (a) The conceptual scattering model. Inset: molecular decomposition centers in glass. Reprinted with permission from a study by Lancry et al. [110] ©Wiley, (b) Feedback-driven evolution of nano-gratings. (c) Experimental proof of nano-gratings. (d) Simulation results or ordered array of carrier layers in bulk fused silica [118].

generation of more or less ordered standing wave periodic patterns resulting from the coherent superposition of scattered waves induced by nanoplasmas or other nuclei. Again, the near-field interaction plays a preponderant role. The evanescent part confines energy and determines locally nanocavitation phenomena at the field maxima. The mutual interaction between light and topography will set in place the pulse-by-pulse feedback, enhancing order with every incoming pulse. As in case of surface interaction (and a similar nature was pointed out between these two types of matter arrangements [117]), an interrogation can be made with respect to the nature of the scattering centers, and we make the hypothesis that they relate to nucleation centers of material decomposition [110]. The scenario is illustrated in Figure 9(a–d), with Figure 9(a) giving the conceptual scattering scheme, Figure 9(b) emphasizing the feedback growth of ordered nanogratings with the laser dose, Figure 9(c) showing an experimentally detected profile, and Figure 9(d) presenting a simulation result of an ordered array of excited carrier layers in bulk fused silica [118]. A more detailed discussion is presented in a study by Stoian et al. [119]. We point out here the capacity to achieve, by light-matter self-organization, characteristic sizes of 100 nm. The correlation with the presence of scattering centers is reinforced in porous materials where singular tight field focusing concentrations were reported down to the definition of single feature nanogratings [28]. A fracture

mechanism (material response) for the nanogratings upon field concentration implies transverse fracture dimensions in the 10 nm range.

The situation can be extrapolated to metal-doped glasses where, beside ionization, laser radiation will trigger a photochemical chain of events, agglomerating ions into nanoparticles [120], and creating a 3D self-organization effect of nanoparticles aligned in the field [121]. The volume field action on spatial arrangements is not limited to nanogratings self-organization. Spatial field distortions and interferential effects in the vicinity of interfaces determine the onset of regular linear (axial) arrays of nanovoids [122]. Further concepts of nanoscale localization in dielectric materials and specifically on thin films was proposed by Kumar et al. [123], where Fabry-Perot interference effect due to index contrast will cleave films at precise, wavelength-defined locations.

5 Observation and control: dynamic coupling between light and matter

The challenge of a laser structuring process is to achieve control over the yield, aspect form, the quality, and the throughput of the process. This becomes even more

challenging when scales hardly accessible by optical means are required. Therefore, in situ and accurate observation means are essential to understand and control laser nanostructuring. The field of laser-matter interaction has largely benefited from time-resolved investigation and rapid monitoring techniques. They have targeted electronic dynamics during and after the passage of the laser pulse, the evolution of the electronic and the vibrational systems in the excited solid exposed to intense fields, the interaction between electronic excitation and structural behavior, the thermomechanical evolution of the excited mater, the development of extraordinary optical and thermal properties on transient scales. The most advanced methods offer the possibility to sample the dynamics of electronic bands or to observe matter movement with atomic resolution [124, 125]. In this rich landscape of methods and strategies, we will mainly focus on the observation of the laser structuring process. Several methods where established, either aiming for temporal or for spatial resolution. The most straightforward method originates in direct imaging with the abovementioned resolution drawbacks concerning optical methods. Nevertheless, due to their easy-to-implement character, optical imaging methods were among the first to be employed, and they concern both surfaces and bulk, for direct nanostructuring, as well as for self-organizational effects.

Time-resolved optical imaging of laser-generate ripples [126, 127] in spite of a difficulty caused by the necessary feedback that relies on multipulse approach, puts into evidence a growth response of tens of ps for the formation of close-to-wavelength LIPSSs, indicating a potential nature evolving from melt hydrodynamics. In a different regime of probing wavelengths, high-resolution time-resolved X-ray studies allowed to visualized dynamically single shot material organization after laser exposure, witnessing already far-field signatures of the onset of periodic topographies [128]. The search for resolution was followed by applying super-resolved microscopy techniques [129]. Visualizing the impacted area during sequential irradiation permitted to observe the phase stability of the nanoscale pattern, establishing a field-related origin. The question of light localization as a function of the topography was recently illustrated using photoemission electron microscopy, revealing regions of field confinement and enhancement on rippled topographies [130]. The correlation between light distribution and evolving topographies in the laser area becomes critical for laser nanostructuring based on light-driven self-organization. Supported by simulations, high-resolution imaging shows that absorption of light on an evolving surface relief drives the selection of the final periodicity, emphasizing the

contributions of radiative and nonradiative scattered fields, as well as the dipole-dipole coupling between scattering centers. Alongside resolution, accessing full optical properties of nanostructures becomes of paramount importance and quantitative optical methods are emerging for the study of nano-objects [131].

In the bulk, ultrafast and multiscale high-resolution imaging techniques were applied to visualize nanoscale-void formation [108], permitting to propose a liquid-supported cavitation scenario in silica glass. A plethora of thermomechanical effects were indicated with the emergence of pressure waves [132] in the aftermath of plasma relaxation close to microexplosion conditions [133]. Alternative methods are based on scattering and diffraction techniques with capabilities to observe nanoscale structures, as first applied on surfaces [134, 135]. Direct diffraction techniques were used either to steer open optimization loops on bulk nanogratings [136] or to detect the dynamic onset of a diffractive response of laser-induced regular structures [137]. X-ray scattering was applied to tomographically reconstitute 3D nanoscale arrangements in the bulk [138, 139], permitting to observed the first steps of the 3D arrangement. Alongside visualization experiments taking advantage of high spatial and temporal resolutions, modeling of the formation of nanoscale structure plays a fundamental role. We particularly emphasize the impact of multiphysical approaches coupling light and electromagnetism with a multiscale material response (electronic, atomic, macroscopic).

The ability to observe processing results facilitated at the same time the implementation of techniques of advanced control based on temporal beam engineering and steering algorithms [140–142] and on spatially regulated beam delivery [143–145]. First, besides geometrical aspects, a time control of irradiation implies regulation of energy deposition. Laser structuring is a complex multiphysical process, where the energy flow should be regulated in order to achieve yield and desired scales. In view of the physical elements leading to extreme processing scales, optimal control strategies were already taken into account, based on the ansatz that among different competitive relaxation channels an optimum can be defined. Balance of nonlinear photoionization mechanism using temporal pulse shaping with asymmetric envelope was already proposed by Englert et al. [34], fostering a situation where excitation peaks can be amplified using spatially selective additional collisional multiplication. For a Gaussian envelope, the mechanism becomes effective only at the peak, confining above threshold excitation in a 100-nm region. Light-driven self-assembling processes are equally sensitive to pulse shapes. Transitions to order and

ripples topographies were found to be sensitive to the excitation rate in view of the transient optical properties of the material [146–148]. Double pulse excitation schemes with variable polarization were applied to achieve a multitude of spatial structure patterns [149–151] and record light confinement [101]. A large range of hierarchical arrangements were then demonstrated [152]. Spectral synthesis of fields using time-separated pulses with different colors [153] can impose order and periodicities related in a material-dependent way to the color content of the pulses and the respective orientations of the fields. Thus, control can be exercised on orientation, size, period, and alignment of topographical structures.

In volume open loops based on pulse envelope control have led to an increased degree of order of 3D nanogratings arrangements [136]. Stretching the pulse in time allows for better nonlinearity control and stronger confinement of radiation, achieving higher energy deposition rates. Double pulse burst schemes were used to improve the birefringence associated with nanogratings [154]. These results show a strong correlation between material morphologies and the rate of energy deposition, indicating that extended control can be achieved over how the material responds to the energy input. Further action will originate in manipulating the vectorial character of the beam in time, guiding thus the direction of the field on surfaces [155] and in interaction with nano-objects [156]. Besides vectorial and temporal coupling, other degrees of freedom emerge from the manipulation of spatial phase properties. Applying propagation corrections and controlling the focal geometries [157, 158] extrapolated to tight focusing will permit better control on the excitation gradients. Beyond the engineering of the shape of the focal plane [159], spatial phase control impacts particularly the field pattern in multibeam interference setups, determining flexibility in the pattern definition and hierarchical arrangements [160].

Further progress was achieved by employing a particular class of beams with strong resistance to nonlinearities, nondiffractive beams, and among them, zero-order Bessel beams. Volume interaction with nondiffractive beams has thus led in the recent years to a robust nanostructuring technique [13, 119, 161]. Adding to this feature the possibility to engineer dispersion via spectral phase modulation, extreme void-like structures with high aspect ratio and nanoscale transverse profiles can be obtained. Beams with topological charge were equally studied for ablation purposes [162]. In addition, the polarization sensitivity has led to the application of vector beams to obtain nonstandard arrangements on surfaces and in the bulk, among them arrangements with particular rotation symmetry [136, 163, 164].

Resuming the above discussion, Figure 10 shows relevant examples of probing and control, with Figure 10(a) indicating in situ super-resolution imaging, Figure 10(b) showing a transient microscopy image of forming ripples at 50 ps after the arrival of the excitation pulse [127], and Figure 10(c) giving an X-ray tomographic fingerprint of emerging 3D self-organization patterns [138]. Examples of electronic and atomistic simulation of structural and morphology changes are given in Figure 10(d) [92, 165]. Building on the dynamic knowledge, pulse engineering techniques may be applied to guide and confine light on corrugated surfaces and in the bulk (Figure 10(e) [164]). Time-resolved optical imaging of the dynamics of volume nanostructuring is shown in Figure 10(f) [108] (transient stages for void generation in glass) together with double pulse multiburst schemes to control order in 3D nanogratings (Figure 10(g) [154]). These example show the capability to observe beyond the optical resolution the evolution of matter during the process in its fastest stages, to simulate the processes from the atom to the macroscale, to control and reconstruct the arrangement of nanostructures, delivering extended knowledge on the nanostructuring process. This capacity of structuring permits the development of a range of related applications in a variety of fields.

6 Nanoscale and function: emerging opportunities in application fields

The application fields of laser generated nanostructures are large and diverse. Performant functions in optics, mechanics, biology emerge from structuring in the range of the optical wavelength, originating in properties defined by topography, specific surface, or feature size. These have been the object of several publications [166–171] and will only be briefly recalled here, outlining a few prominent application fields. The upgrade potentially offered by sub-100-nm is under scrutiny and forecasts a tremendous potential as the material response to solicitation becomes quasi-resonant with the structuring scale. A major development axis is related to biomimetics, where a texture pattern originates from natural examples of extraordinary behaviors. Inspired by nature or created by design, functions related to laser multiscale microstructuring and nanostructuring were demonstrated to be effective in major fields covering mechanics, life sciences, energy, and optics. Case of relevant functions is illustrated for each field in Figure 11.
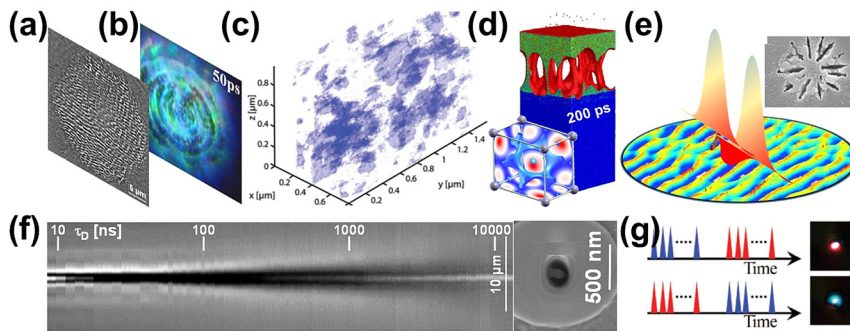
Figure 10: (a) Structured illumination microscopy for in situ imaging of nanostructured surfaces [129]. (b) Transient microscopy image of forming ripples at 50 ps after the onset of the excitation pulse. Reprinted with permission from a study by Jia et al. [127] ©American Institute of Physics. (c) X-ray tomographic reconstruction of 3D embedded nanostructures. Reprinted with permission from a study by Richter et al. [138] ©Wiley. (d) Example of modeling electronic and molecular response of materials [92, 165]. (e) Pulse engineering and feedback driven surface topographies. Inset: Arrangement of nanogratings with azimuthally polarized beams. Reprinted with permission from a study by Hnatovsky et al. [164] ©American Physical Society. (f) Time-resolved optical imaging of cavitation in glass [108]. (g) Double pulse multi-burst sequences to control 3D nanogratings and the associated birefringence. Reprinted with permission from a study by Shimotsuma et al. [154] ©Wiley.
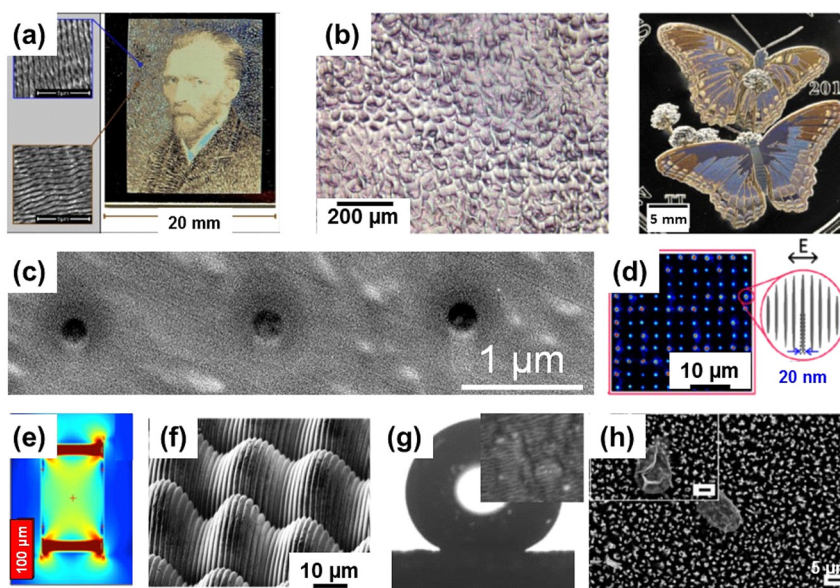
Figure 11: Functionalities of laser-induced nanostructures.
(a) Structural colors and optical marking using laser-induced periodic surface structure (LIPSS). Reprinted with permission from a study by Dusser et al. [172] ©The Optical Society. (b) Plasmonic colors from laser ablation nanoparticles. Reprinted with permission from a study by Guay et al. [173] ©Nature. (c) Volume nanostructuring with Bessel beams for waveguide Bragg gratings [174]. (d) Encoding and data storage in nanogratings domains embedded in glass. Reprinted with permission from a study by Zhang et al. [175] ©American Physical Society. (e) Stress control using laser nanostructured domains. Reprinted with permission from a study by McMillen et al. [176] ©The Optical Society. (f) Biomimetic hierarchical structures reprinted with permission from a study by Lasagni et al. [160] ©MDPI. (g) Superhydrophobic contact properties originating in hierarchical topographies. Reprinted with permission from a study by Jiao et al. [177] ©MDPI. (h) Bactericide properties of nanostructured surfaces. Reprinted with permission from a study by Ivanova et al. [178] ©Nature.

Staying with the optical domain, we will give below two examples, the definition of structural and plasmonic colors and the photon harvesting effect by light trapping at interfaces. The first application field is represented in Figure 11(a,b). It refers to the diffractive effect of regular nanostructures resulting in chromaticity, as well as to the potential plasmonic resonances of nanosized particles. The periodicities, orientation, and their sizes render control on color organization and appearance, providing thus an optical marking effect [172, 173, 179], transferring information to color. The feature scale smaller the the wavelength can sample and scatter the optical field and create further effects, among them the generation of antireflective properties [25, 180, 181]. Laser-induced microcone-like structures on semiconductors [24, 182] (see example in Figure 1(k)), similar to what can be produced by reactive etching, outperform current capacities for harvesting photons for sensors and photovoltaic applications, showing increased absorptivity down to the infrared spectral domain [183]. The effect is based on multiple reflections on the cones trapping light and increasing absorption; the local field enhancement induces equally electronic emission, interesting for field emitters. Besides the direct landscape effects, additional properties originate from the degree of order or disorder. Further light localization effects on randomly nanostructured interfaces were demonstrated to enhance absorption via Anderson localization [184]. Capacities to laser structure on the 100-nm scale are already on development, enlarging the spectral window of effectiveness.

In three dimensions, the capacity of nanomorphing enables to sample, readout, and manipulate the optical field in embedded photonic circuits and to create optical resonances sensitive to environments, for example, temperature, pressure, and chemical fields (see [185] and references therein). Recently, the use of highly confining nondiffractive beams was demonstrated to achieve high aspect ratio structures with sections in the 100-nm range [174], generating strong Bragg resonances for temperature and stress measurements. An example of the nanostructured Bragg grating area is given in Figure 11(c). Three-dimensional arrangements of nanoparticles and nanoscale-topographies can develop color properties to encrypt information [186]. Three-dimensional memories are demonstrated by 3D positioning of nanoparticle domains or nanogratings [175, 187], where the latter couples positioning and orientational degrees of freedom to create high density storage in long-life supports (Figure 11(d)). The generation of embedded nanostructures can equally produce stress constraints, serving as movement actuators [176] (Figure 11(e)).

Mechanical and contact functions count among the most impressive functionalities generated by nanostructured surfaces and volumes. Inspired by nature, hierarchical design (Figure 11(f)) can be applied to control surfactant properties, for example, the wetting properties of a surface, from hydrophilicity to hydrophobicity. The effect of topography on defining surface properties and contact angles [188, 189] by engineering interfacial energy and surface tension were recently revisited in a study by Müller et al. [171]. Coupling topography and chemistry (notably oxidation during the fabrication process [190] but also long-term adsorbents and contamination, with a prospect for light-assisted chemistry at nanostructured surfaces [191]), superhydrophobic surfaces can be generated [25, 181]. An example is given in Figure 11(g), showing a laser-treated part issued from additive manufacturing [177] with hydrophobic properties. In many cases, the superhydrophobicity resulting from nanoroughness can be associated with transparency or antireflective properties of surfaces [25, 192]. Further functions are expected to influence adhesion, sliding, or friction, and, at the same time, interfacial flow and fluidics. Last but not the least, structuring on the nanoscale can impact biological behavior and we resume this discussion with an extension of structuring to induce tribological stress for living tissues and organisms; a bactericide effect on a nanostructured surface [178] is depicted in Figure 11(h). A nanostructured surface can have a far reaching effect in, e.g., preservation and storage of cells, in transduction of biological materials, or in tissue engineering. At the same time, the capacity to focus opened up new opportunities in nanosurgery [193, 194], biocompatibility [195], and cell transfection [196, 197]. Further nanoscale aspects can be noted in generation of nanoparticles and foams for a diverse range of applications.

7 Conclusions and outlook

In a competitive context with significant economic opportunities, ultrafast laser structuring is steadily evolving to a precise, rapid, and ecologically friendly micro-nano fabrication technology, creating the premises of an industrial leap forward. Applications and industrial fabrication means have already emerged for structuring surfaces and volumes on a micron scale, with submicrometer precision, notably in tribology, biocompatibility, or optics. The sub-100-nm scale is an enabling dimension toward a new class of functions, where notably resonances between structure and properties are developed, at the border between quantum and mesoscopic physics. Access to sub-100-nm scales will define the

new generation of laser processing technologies. It requires nevertheless extensive physical knowledge and control means, prospecting a situation where the required function will derive from a combination of topography, morphology, and chemistry. This frame will link structural size to pattern, pattern to function, and function to performance. We have reviewed here main physical processes and conditions leading to structuring on extreme scales using remote optical beams. It is difficult to imagine the full extent of concepts concurring for nanostructuring, from optical engineering and advanced sources to self-assembly properties. The message we would like to deliver in this quest against diffraction is nevertheless to harness, in addition to light, the material reaction as a direct means to bypass optical limits. The field is advancing at fast pace. The advent of new attosecond XUV technologies with high photon flux will create new options and opportunities for irradiation and imaging. Potential emerges equally from the combination of multispectral fields mixing large and short wavelengths, where independent excitation channels become mutually assisted. Yield and resolution are thus matched. Spectral, vectorial, and time-controlled optimal interaction concepts are about to emerge driven by the last developments in computer-assisted strategies. Advances are equally made in terms of accurate and precise processing sources, workstations, and environments with automated computer-aided design and manufacturing (CAD/CAM) potentialities. An accurate process requires an accurate vision and in situ monitoring necessitates now techniques that associate high-resolution with large field view. Concepts inspired from super-resolution microscopy or ptychography, combining fast algorithms and coherence engineering with quantitative measurements will determine a leap forward in the future laser nanotechnologies. The potential of laser for extreme nanostructuring is considerable, and we just note its amazing development from the moment it was created as "a solution seeking a problem".

References

[1] T. H. Maiman, "Stimulated optical radiation in ruby," *Nature*, vol. 187, p. 493, 1960.

[2] F. Brech and L. Cross, "Optical microemission stimulated by a ruby maser," *Appl. Spectrosc.*, vol. 16, p. 59, 1962.

[3] R. E. Honig and J. R. Woolston, "Laser induced emission of electrons, ions, and neutral atoms from solid surfaces," *Appl. Phys. Lett.*, vol. 2, pp. 138–139, 1963.

[4] R. C. Rosan, M. K. Healy, and W. F. McNary, Jr., "Spectroscopic ultramicroanalysis with a laser," *Science*, vol. 142, pp. 236–237, 1963.

[5] J. R. Nall and J. W. Lathrop, "Photolithographic fabrication techniques for transistors which are an integral part of a printed circuit," *IEEE Trans. Electron. Dev.*, vol. 5, p. 117, 1958.

[6] J. C. Miller, *Laser Ablation: Principles and Applications, Springer Series in Materials Science*, 26, Berlin, Springer-Verlag, 1994.

[7] E. Abbe and H. Lawson, Eds. Translated by Fripp HE. "A contribution to the theory of the microscope and the nature of microscopic vision," *Proceedings of the Bristol Naturalists' Society*, vol. 1, London, UK, Williams & Northgate, 1876, pp. 200–261.

[8] L. Rayleigh, "Investigations in optics, with special reference to the spectroscope," *Philos. Mag.*, vol. 8, pp. 261–274, 1879.

[9] P. P. Pronko, S. K. Dutta, J. Squier, J. V. Rudd, D. Du, and G. Mourou, "Machining of sub-micron holes using a femtosecond laser at 800 nm," *Opt. Commun.*, vol. 114, pp. 106–110, 1995.

[10] S. Nolte, B. N. Chichkov, H. Welling, Y. Shani, K. Lieberman, and H. Terkel, "Nanostructuring with spatially localized femtosecond laser pulses," *Opt. Lett.*, vol. 24, pp. 914–916, 1999.

[11] A. P. Joglekar, H. Liu, E. Meyhöfer, G. Mourou, and A. J. Hunt, "Optics at critical intensity: applications to nanomorphing," *Proc. Natl. Acad. Sci. U. S. A.*, vol. 101, pp. 5856–5861, 2004.

[12] Y. V. White, X. Li, Z. Sikorski, L. M. Davis, and W. Hofmeister, "Single-pulse ultrafast-laser machining of high aspect nano-holes at the surface of SiO_2," *Opt. Express*, vol. 16, pp. 14413–14420, 2008.

[13] M. K. Bhuyan, F. Courvoisier, P. A. Lacourt, et al., "High aspect ratio nanochannel machining using single shot femtosecond Bessel beams," *Appl. Phys. Lett.*, vol. 97, p. 08110, 2010.

[14] P. Simon and J. Ihlemann, "Machining of submicron structures on metals and semiconductors by ultrashort UV-laser pulse," *Appl. Phys. A Mater. Sci. Process*, vol. 63, pp. 505–508, 1996.

[15] J. B. Pelka, R. Sobierajski, D. Klinger, et al., "Damage in solids irradiated by a single shot of XUV free-electron laser: irreversible changes investigated using X-ray microdiffraction, atomic force microscopy and Nomarski optical microscopy," *Radiat. Phys. Chem.*, vol. 78, pp. S46–S52, 2009.

[16] K. Sakaue, H. Motoyama, R. Hayashi, et al., "Surface processing of PMMA and metal nano-particle resist by sub-micrometer focusing of coherent extreme ultraviolet high-order harmonics pulses," *Opt. Lett.*, vol. 45, pp. 2926–2929, 2020.

[17] A. Chimmalgi, C. P. Grigoropoulos, and K. Komvopoulos, "Surface nanostructuring by nano-/femtosecond laser-assisted scanning force microscopy," *J. Appl. Phys.*, vol. 97, p. 104319, 2005.

[18] Y. N. Kulchin, O. B. Vitrik, A. A. Kuchmizhak, et al., "Through nanohole formation in thin metallic film by single nanosecond laser pulses using optical dielectric apertureless probe," *Opt. Lett.*, vol. 38, pp. 1452–1454, 2013.

[19] D. S. Ivanov, A. I. Kuznetsov, V. P. Lipp, et al., "Short laser pulse nanostructuring of metals: direct comparison of molecular dynamics modeling and experiment," *Appl. Phys. A Mater. Sci. Process*, vol. 111, pp. 675–687, 2013.

[20] A. Khan, Z. Wang, M. A. Sheikh, D. J. Whitehead, and L. Li, "Laser micro/nano patterning of hydrophobic surface by contact particle lens array," *Appl. Surf. Sci.*, vol. 258, pp. 774–779, 2011.

[21] J. H. Klein-Wiele and P. Simon, "Sub-wavelength pattern generation by laser direct writing via repeated irradiation," *Opt. Express*, vol. 21, pp. 626–630, 2013.

[22] M. Garcia-Lechuga, D. Puerto, Y. Fuentes-Edfuf, J. Solis, and J. Siegel, "Ultrafast moving-spot microscopy: birth and growth of laser-induced periodic surface structures," *ACS Photonics*, vol. 3, pp. 1961–1967, 2016.

[23] C. S. R. Nathala, A. Ajami, A. A. Ionin, et al., "Experimental study of fs-laser induced sub-100-nm periodic surface structures on titanium," *Opt. Express*, vol. 23, pp. 5915–5929, 2015.

[24] T. H. Her, R. J. Finlay, C. Wu, S. Deliwala, and E. Mazur, "Microstructuring of silicon with femtosecond laser pulses," *Appl. Phys. Lett.*, vol. 73, pp. 1673–1675, 1998.

[25] A. Papadopoulos, E. Skoulas, A. Mimidis, et al., "Biomimetic omnidirectional antireflective glass via direct ultrafast laser nanostructuring," *Adv. Mater.*, vol. 31, p. 1901123, 2019.

[26] A. Y. Vorobyev and C. Guo, "Femtosecond laser nanostructuring of metals," *Opt. Express*, vol. 14, pp. 2164–2169, 2006.

[27] Y. Shimotsuma, P. G. Kazansky, L. Qiu, and K. Hirao, "Self-organized nanogratings in glass irradiated by ultrashort light pulses," *Phys. Rev. Lett.* vol. 91, p. 247405, 2003.

[28] Y. Liao, Y. Cheng, C. Liu, et al., "Direct laser writing of sub-50 nm nanofluidic channels buried in glass for three-dimensional micro-nanofluidic integration," *Lab Chip*, vol. 13, pp. 1626–1631, 2013.

[29] P. K. Velpula, M. K. Bhuyan, F. Courvoisier, H. Zhang, J. P. Colombier, and R. Stoian, "Spatio-temporal dynamics in nondiffractive Bessel ultrafast laser nanoscale volume structuring," *Laser Photonics Rev.*, vol. 2, pp. 230–244, 2016.

[30] M. Malinauskas, M. Farsari, A. Piskarskas, and S. Juodkazis, "Ultrafast laser nanostructuring of photopolymers: a decade of advances," *Phys. Rep.*, vol. 533, pp. 1–31, 2013.

[31] C. Doñate-Buendía, M. Fernández-Alonso, J. Lancis, and G. Mínguez-Vega, "Overcoming the barrier of nanoparticle production by femtosecond laser ablation in liquids using simultaneous spatial and temporal focusing," *Photonics Res.*, vol. 7, pp. 1249–1257, 2019.

[32] N. Shen, D. Datta, C. B. Schaffer, P. LeDuc, D. E. Ingber, and E. Mazur, "Ablation of cytoskeletal filaments and mitochondria in cells using a femtosecond laser nanoscissor," *Mol. Cell. Biomech.*, vol. 2, pp. 17–25, 2005.

[33] C. T. A. Brown, D. J. Stevenson, X. Tsampoula, et al., "Enhanced operation of femtosecond lasers and applications in cell transfection," *J. Biophotonics*, vol. 3, pp. 183–199, 2008.

[34] L. Englert, B. Rethfeld, L. Haag, M. Wollenhaupt, C. Sarpe-Tudoran, and T. Baumert, "Control of ionization processes in high band gap materials via tailored femtosecond pulses," *Opt. Express*, vol. 15, pp. 17855–17862, 2007.

[35] D. Bäuerle, *Laser Processing and Chemistry*, Berlin Heidelberg, Springer-Verlag, 2011.

[36] R. Weber, T. Graf, P. Berger, et al., "Heat accumulation during pulsed laser materials processing," *Opt. Express*, vol. 22, pp. 11312–11324, 2014.

[37] R. Le Harzic, N. Huot, E. Audouard, et al., "Comparison of heat-affected zones due to nanosecond and femtosecond laser pulses using transmission electronic microscopy," *Appl. Phys. Lett.*, vol. 80, pp. 3886–3888, 2002.

[38] A. I. Kuznetsov, J. Koch, and B. N. Chichkov, "Nanostructuring of thin gold films by femtosecond lasers," *Appl. Phys. A Mater. Sci. Process*, vol. 94, pp. 221–230, 2009.

[39] Y. P. Meshcheryakov and N. M. Bulgakova, "Thermoelastic modeling of microbump and nanojet formation on nanosize gold films under femtosecond laser irradiation," *Appl. Phys. A Mater. Sci. Process*, vol. 82, pp. 363–368, 2006.

[40] Q. Li, D. Grojo, A. P. Alloncle, B. Chichkov, and P. Delaporte, "Digital laser micro- and nanoprinting," *Nanophotonics*, vol. 8, pp. 27–44, 2019.

[41] T. E. Itina, "On nanoparticle formation by laser ablation in liquids," *J. Phys. Chem. C*, vol. 115, pp. 5044–5048, 2010.

[42] H. Zeng, X. W. Du, S. C. Singh, et al., "Nanomaterials via laser ablation/irradiation in liquid: a review," *Adv. Funct. Mater.*, vol. 22, pp. 1333–1353, 2012.

[43] D. Zhang, B. Gökce, and S. Barcikowski, "Laser synthesis and processing of colloids: fundamentals and applications," *Chem. Rev.*, vol. 117, pp. 3990–4103, 2017.

[44] M. Garcia-Lechuga, O. Utéza, N. Sanner, and D. Grojo, "Evidencing the nonlinearity independence of resolution in femtosecond laser ablation," *Opt. Lett.*, vol. 45, pp. 952–955, 2020.

[45] D. Ashkenasi, A. Rosenfeld, H. Varel, M. Wähmer, and E. E. B. Campbell, "Laser processing of sapphire with picosecond and sub-picosecond pulses," *Appl. Surf. Sci.*, vol. 120, pp. 65–80, 1997.

[46] A. Ródenas, M. Gu, G. Corrielli, et al., "Three-dimensional femtosecond laser nanolithography of crystals," *Nat. Photonics*, vol. 13, pp. 105–109, 2019.

[47] D. E. Grady, "The spall strength of condensed matter," *J. Mech. Phys. Solids.*, vol. 36, pp. 353–384, 1988.

[48] A. Vogel, J. Noack, G. Hüttman, and G. Paltauf, "Mechanisms of femtosecond laser nanosurgery of cells and tissues," *Appl. Phys. B Laser Opt.*, vol. 81, pp. 1015–1047, 2005.

[49] J. B. Pendry, "Negative refraction makes a perfect lens," *Phys. Rev. Lett.*, vol. 85, pp. 3966–3968, 2000.

[50] D. F. Sievenpiper, M. E. Sickmiller, and E. Yablonovitch, "3D wire mesh photonic crystals," *Phys. Rev. Lett.*, vol. 76, pp. 2480–2482, 1996.

[51] V. G. Veselago, "The electrodynamics of substances with simultaneously negative and μ," *Sov. Phys. Usp.*, vol. 10, pp. 509–514, 1968.

[52] F. Qin, K. Huang, J. Wu, J. Teng, C. W. Qiu, and M. Hong, "A Supercritical lens optical label-free microscopy: sub-diffraction resolution and ultra-long working distance," *Adv. Mater.*, vol. 29, p. 1602721, 2017.

[53] K. Mishchik, Y. Petit, E. Brasselet, A. Royon, T. Cardinal, and L. Canioni, "Patterning linear and nonlinear optical properties of photosensitive glasses by femtosecond structured light," *Opt. Lett.*, vol. 40 pp. 201–204, 2014.

[54] I. Falcón Casas and W. Kautek, "Subwavelength nanostructuring of gold films by apertureless scanning probe lithography assisted by a femtosecond fiber laser oscillator," *Nanomaterials*, vol. 8, p. 536, 2018.

[55] F. Korte, S. Nolte, B. N. Chichkov, et al., "Far-field and near-field material processing with femtosecond laser pulses," *Appl. Phys. A Mater. Sci. Process*, vol. 69, pp. S7–S11, 1999.

[56] X. Sedao, T. J. Y. Derrien, G. R. B. E. Romer, B. Pathiraj, and A. J. Huis in't Veld, "Large area laser surface micro/nanopatterning by contact microsphere lens arrays," *Appl. Phys. A Mater. Sci. Process*, vol. 111, pp. 701–709, 2013.

[57] T. Kondo, S. Matsuo, S. Juodkazis, V. Mizeikis, and H. Misawa, "Multiphoton fabrication of periodic structures by multibeam interference of femtosecond pulses," *Appl. Phys. Lett.*, vol. 82, pp. 2758–2760, 2003.

[58] G. M. Burrow and T. K. Gaylord, "Multi-beam interference advances and applications: nano-electronics, photonic crystals, metamaterials, subwavelength structures, optical trapping, and biomedical structures," *Micromachines*, vol. 2, pp. 221–257, 2011.

[59] E. Betzig and J. K. Trautman, "Near-field optics: microscopy, spectroscopy, and surface modification beyond the diffraction Limit," *Science*, vol. 257, pp. 189–195, 1992.

[60] M. Terakawa, S. Takeda, Y. Tanakaa, et al., "Enhanced localized near field and scattered far field for surface nanophotonics applications," *Prog. Quant. Electr.*, vol. 36, pp. 194–271, 2012.

[61] K. Piglmayer, R. Denk, and D. Bäuerle, "Laser-induced surface patterning by means of microspheres," *Appl. Phys. Lett.*, vol. 80, pp. 4693–4695, 2002.

[62] D. Brodoceanu, L. Lanström, and D. Bäuerle, "Laser-induced nanopatterning of silicon with colloidal monolayers," *Appl. Phys. A*, vol. 86, pp. 313–314, 2007.

[63] N. Nedyalkov, T. Sakai, T. Miyanishi, and M. Obaraa, "Near field distribution in two dimensionally arrayed gold nanoparticles on platinum substrate," *Appl. Phys. Lett.*, vol. 90, p. 123106, 2007.

[64] F. Hubenthal, R. Morarescu, L. Englert, L. Haag, T. Baumert, and F. Träger, "Parallel generation of nanochannels in fused silica with a single femtosecond laser pulse: exploiting the optical near fields of triangular nanoparticles," *Appl. Phys. Lett.*, vol. 95, p. 063101, 2009.

[65] E. Mcleod and C. Arnold, "Subwavelength direct-write nanopatterning using optically trapped microspheres," *Nat. Nanotechnol.*, vol. 3, pp. 413–417, 2008.

[66] Z. Wang, W. Guo, L. Li, et al., "Optical virtual imaging at 50 nm lateral resolution with a white-light nanoscope," *Nat. Commun.*, vol. 2, p. 218, 2011.

[67] S. Lecler, S. Perrin, A. Leong-Hoi, and P. Montgomery, "Photonic jet lens," *Sci. Rep.*, vol. 9, p. 4725, 2019.

[68] M. Mosbacher, H. J. Münzer, J. Zimmermann, J. Solis, J. Boneberg, and P. Leiderer, "Optical field enhancement effects in laser-assisted particle removal," *Appl. Phys. A Mater. Sci. Process*, vol. 72, pp. 41–44, 2001.

[69] K. Kawamura, N. Sarukura, M. Hirano, N. Ito, and H. Hosono, "Periodic nanostructure array in crossed holographic gratings on silica glass by two interfered infrared-femtosecond laser pulses," *Appl. Phys. Lett.*, vol. 79, pp. 1228–1230, 2001.

[70] Z. Z. Li, L. Wang, H. Fan, et al., "far-field-induced near-field breakdown for direct nanowriting in an atmospheric environment," *Light Sci. Appl.*, vol. 9, p. 41, 2020.

[71] J. F. Young, J. S. Preston, H. M. van Driel, and J. E. Sipe, "Laser-induced periodic surface structure. II. Experiments on Ge, Si, Al, and brass," *Phys. Rev. B*, vol. 27, pp. 1155–1172, 1983.

[72] J. Bonse and S. Gräf, "Maxwell meets Marangoni—a review of theories on laser-induced periodic surface structures," *Laser Photonics Rev*, p. 2000215, 2020, https://doi.org/10.1002/lpor.202000215.

[73] M. Birnbaum, "Semiconductor surface damage produced by ruby lasers," *J. Appl. Phys.*, vol. 36, pp. 3688–3689, 1965.

[74] R. Buividas, M. Mikutis, and S. Juodkazis, "Surface and bulk structuring of materials by ripples with long and short laser pulses: recent advances," *Prog. Quant. Electr.*, vol. 38, pp. 119–156, 2014.

[75] J. E. Sipe, J. F. Young, J. S. Preston, and H. M. van Driel, "Laser-induced periodic surface structure. I. Theory," *Phys. Rev. B*, vol. 27, pp. 1141–1154, 1983.

[76] J. Bonse, A. Rosenfeld, and J. Krüger, "On the role of surface plasmon polaritons in the formation of laser-induced periodic surface structures upon irradiation of silicon by femtosecond-laser pulses," *J. Appl. Phys.*, vol. 106, p. 104910, 2009.

[77] O. Varlamova, F. Costache, J. Reif, and M. Bestehorn, "Self-organized pattern formation upon femtosecond laser ablation by circularly polarized light," *Appl. Surf. Sci.*, vol. 252, pp. 4702–4706, 2006.

[78] O. Varlamova, J. Reif, S. Varlamov, M. Bestehorn and , "The laser polarization as control parameter in the formation of laser-induced periodic surface structures: comparison of numerical and experimental results." *Appl. Surf. Sci.*, vol. 257 pp. 5465–5469, 2011.

[79] M. Castro, R. Cuerno, L. Vázquez, and R. Gago, "Self-organized ordering of nanostructures produced by ion-beam sputtering," *Phys. Rev. Lett.*, vol. 94, p. 016102, 2005.

[80] V. I. Emel'yanov, "Kuramoto-Sivashinsky equation for modulation of surface relief of molten layer and formation of surface periodic microstructures under pulsed laser irradiation of solids," *Laser Phys.*, vol. 21, pp. 222–228, 2011.

[81] A. M. Turing, "The chemical basis of morphogenesis," *Phil. Trans. R. Soc. Lond. B*, vol. 237, pp. 37–72, 1952.

[82] G. D. Tsibidis, E. Skoulas, A. Papadopoulos, and E. Stratakis, "Convection roll-driven generation of supra-wavelength periodic surface structures on dielectrics upon irradiation with femtosecond pulsed lasers," *Phys. Rev. B*, vol. 94, p. 081305(R), 2016.

[83] E. L. Gurevich, Y. Levy, S. V. Gurevich, and N. M. Bulgakova, "Role of the temperature dynamics in formation of nanopatterns upon single femtosecond laser pulses on gold," *Phys. Rev. B*, vol. 95, p. 054305, 2017.

[84] B. Öktem, I. Pavlov, S. Ilday, et al., "Nonlinear laser lithography for indefinitely large area nanostructuring with femtosecond pulses," *Nat. Photonics*, vol. 7, p. 897, 2013.

[85] I. Prigogine, "Time, structure, and fluctuations," *Science*, vol. 201, pp. 777–785, 1978.

[86] C. Brosseau and D. Bicout, "Entropy production in multiple scattering of light by a spatially random medium," *Phys. Rev. E*, vol. 50, p. 4997, 1994.

[87] I. Gnilitskyi, T. J. Y. Derrien, Y. Levy, N. M. Bulgakova, T. Mocek, and L. Orazi, "High-speed manufacturing of highly regular femtosecond laser-induced periodic surface structures: physical origin of regularity," *Sci. Rep.*, vol. 7, p. 8485, 2017.

[88] W. Zhang, G. Cheng, X. D. Hui, and Q. Feng, "Abnormal ripple patterns with enhanced regularity and continuity in a bulk metallic glass induced by femtosecond laser irradiation," *Appl. Phys. A Mater. Sci. Process*, vol. 115, pp. 1451–1455, 2014.

[89] M. Huang, F. L. Zhao, Y. Cheng, N. S. Xu, and Z. Z. Xu, "Origin of laser-induced near-subwavelength ripples: interference between surface plasmons and incident laser," *ACS Nano*, vol. 3, p. 4062, 2009.

[90] L. Wang, X. W. Cao, M. Irfan Abid, et al., "Nano-ablation of silica by plasmonic surface wave at low fluence," *Opt. Lett.*, vol. 42, pp. 4446–4449, 2017.

[91] J. L. Déziel, J. Dumont, D. Gagnon, L. J. Dubé, S. H. Messaddeq, and Y. Messaddeq, "Toward the formation of crossed laser-induced periodic surface structures," *J. Opt.*, vol. 17, p. 075405, 2015.

[92] A. Abou-Saleh, E. T. Karim, C. Maurice, et al., "Spallation-induced roughness promoting high spatial frequency nanostructure formation on Cr," *Appl. Phys. Mater. Sci. Process*, vol. 124, p. 308, 2018.

[93] R. Rudenko, C. Mauclair, F. Garrelie, R. Stoian, and J. P. Colombier, "Self-organization of surfaces on the nanoscale by topography-mediated selection of quasi-cylindrical and plasmonic waves," *Nanophotonics*, vol. 8, pp. 459–465, 2019.

[94] A. Rudenko, A. Abu-Saleh, F. Pigeon, F. Garrelie, R. Stoian, and J. P. Colombier, "High-frequency periodic patterns driven by non-radiative fields coupled with Marangoni convection instabilities on laser-excited surfaces," *Acta Mater.*, vol. 194, pp. 93–105, 2020.

[95] A. M. Bonch-Bruevich, M. N. Libenson, V. S. Makin, and V. V. Trubaev, "Surface electromagnetic waves in optics," *Opt. Eng.*, vol. 31, pp. 718–730, 1992.

[96] P. Lalanne, J. P. Hugonin, H. T. Liu, and B. Wang, "A microscopic view of the electromagnetic properties of sub-λ metallic surfaces," *Surf. Sci. Rep.*, vol. 64, pp. 453–469, 2009.

[97] A. Y. Nikitin, S. G. Rodrigo, F. J. Garca-Vidal, and L. Martn-Moreno, "In the diffraction shadow: norton waves versus surface plasmon polaritons in the optical region," *New J. Phys.*, vol. 11, p. 123020, 2009.

[98] H. Zhang, J. P. Colombier, C. Li, N. Faure, G. Cheng, and R. Stoian, "Coherence in ultrafast laser-induced periodic surface structures," *Phys. Rev. B*, vol. 92, p. 174109, 2015.

[99] X. Sedao, A. Abou-Saleh, A. Rudenko, et al., "Self-arranged periodic nanovoids by ultrafast laser-induced near-field enhancement," *ACS Photonics*, vol. 5, pp. 1418–1426, 2018.

[100] X. Sedao, M. V. Shugaev, C. Wu, et al., "Growth twinning and generation of high-frequency surface nanostructures in ultrafast laser-induced transient melting and resolidification," *ACS Nano*, vol. 10, pp. 6995–7007, 2016.

[101] A. Abou-Saleh, A. Rudenko, S. Reynaud, F. Pigeon, F. Garrelie, and J. P. Colombier, "Sub-100 nm 2D nanopatterning on a large scale by ultrafast laser energy regulation," *Nanoscale*, vol. 12, pp. 6609–6616, 2020.

[102] K. Itoh, W. Watanabe, S. Nolte, and C. Schaffer, "Ultrafast processes for bulk modification of transparent materials," *MRS Bull.*, vol. 31, pp. 620–625, 2006.

[103] D. Tan, K. N. Sharafudeen, Y. Yue, and J. Qiu, "Femtosecond laser induced phenomena in transparent solid materials: fundamentals and applications," *Prog. Mater. Sci.*, vol. 76, pp. 154–228, 2016.

[104] R. Stoian, "Volume photoinscription of glasses: three-dimensional micro- and nanostructuring with ultrashort laser pulses," *Appl. Phys. A*, vol. 126, p. 438, 2020.

[105] E. N. Glezer and E. Mazur, "Ultrafast-laser driven micro-explosions in transparent materials," *Appl. Phys. Lett.*, vol. 71, pp. 882–884, 1997.

[106] S. Juodkazis, K. Nishimura, S. Tanaka, et al., "Laser-induced microexplosion in the bulk of a sapphire crystal: evidence of Mb pressures," *Phys. Rev. Lett.*, vol. 96, p. 166101, 2006.

[107] A. Vailionis, E. G. Gamaly, V. Mizeikis, W. Yang, A. V. Rode, and S. Juodkazis, "Evidence of superdense aluminium synthesized by ultrafast microexplosion," *Nat. Commun.*, vol. 2, p. 445, 2011.

[108] M. K. Bhuyan, M. Somayaji, A. Mermillod-Blondin, F. Bourquard, J. P. Colombier, and R. Stoian, "Ultrafast laser nanostructuring in bulk silica, a "slow" microexplosion," *Optica*, vol. 4, pp. 951–958, 2017.

[109] L. Rapp, R. Meyer, R. Giust, et al., "High aspect ratio micro-explosions in the bulk of sapphire generated by femtosecond Bessel beams," *Sci. Rep.*, vol. 6, p. 34286, 2016.

[110] M. Lancry, B. Poumellec, J. Canning, K. Cook, J. C. Poulin, and F. Brisset, "Ultrafast nanoporous silica formation driven by femtosecond laser irradiation," *Laser Photonics Rev.*, vol. 7, pp. 953–962, 2007.

[111] L. Bressel, D. de Ligny, E. G. Gamaly, A. V. Rode, and S. Juodkazis, "Observation of O_2 inside voids formed in GeO_2 glass by tightly-focused fs-laser pulses," *Opt. Mater. Express*, vol. 1, pp. 1150–1157, 2011.

[112] K. Mishchik, C. D'Amico, P. K. Velpula, et al., "Ultrafast laser induced electronic and structural modifications in bulk fused silica," *J. Appl. Phys.*, vol. 213, p. 133502, 2013.

[113] K. M. Davis, K. Miura, N. Sugimoto, and K. Hirao, "Writing waveguides in glass with a femtosecond laser," *Opt. Lett.*, vol. 21, pp. 1729–1731, 1996.

[114] R. Taylor, H. Hnatovsky, and E. Simova, "Applications of femtosecond laser induced self-organized planar nanocracks inside fused silica glass," *Laser Photonics Rev.*, vol. 2, pp. 26–46, 2008.

[115] R. Buschlinger, S. Nolte, and U. Peschel, "Self-organized pattern formation in laser-induced multiphoton ionization," *Phys. Rev. B*, vol. 89, p. 184306, 2014.

[116] A. Rudenko, J. P. Colombier, and T. E. Itina, "From random inhomogeneities to periodic nanostructures induced in bulk silica by ultrashort laser," *Phys. Rev. B*, vol. 93, p. 075427, 2016.

[117] R. Rudenko, J. P. Colombier, S. Höhm, et al., "Spontaneous periodic ordering on the surface and in the bulk of dielectrics irradiated by ultrafast laser: a shared electromagnetic origin," *Sci. Rep.*, vol. 7, p. 12306, 2017.

[118] G. Cheng, A. Rudenko, C. D'Amico, T. E. Itina, J. P. Colombier, and R. Stoian, "Embedded nanogratings in bulk fused silica under non-diffractive Bessel ultrafast laser irradiation," *Appl. Phys. Lett.*, vol. 110, p. 261901, 2017.

[119] R. Stoian, M. K. Bhuyan, A. Rudenko, J. P. Colombier, and G. Cheng, "High-resolution material structuring using ultrafast laser non-diffractive beams," *Adv. Phys. X*, vol. 4, p. 1659180, 2019.

[120] A. Royon, K. Bourhis, M. Bellec, et al., "Silver clusters embedded in glass as a perennial high capacity optical recording medium," *Adv. Mater.*, vol. 22, pp. 5282–5286, 2010.

[121] N. Crespo-Monteiro, N. Destouches, L. Bois, F. Chassagneux, S. Reynaud, and T. Fournel, "Reversible and irreversible laser microinscription on silver-containing mesoporous titania films," *Adv. Mater.*, vol. 22, pp. 3166–3170, 2010.

[122] S. Kanehira, J. Si, J. Qiu, F. Fujita, K. Hirao, "Periodic nanovoid structures via femtosecond laser irradiation," *Nano Lett.*, vol. 5, pp. 1591–1595, 2005.

[123] K. Kumar, K. K. C. Lee, J. Li, J. Nogami, N. P. Kherani, and P. R. Herman, "Quantized structuring of transparent films with femtosecond laser interference," *Light Sci. Appl.*, vol. 3, p. e157, 2014.

[124] A. Sommer, E. M. Bothschafter, S. A. Sato, et al., "Attosecond nonlinear polarization and light–matter energy transfer in solids," *Nature*, vol. 534, pp. 86–90, 2016.

[125] P. Zalden, F. Quirin, M. Schumacher, et al., "Femtosecond x-ray diffraction reveals a liquid-liquid phase transition in phase-change materials," *Science*, vol. 364, pp. 1062–1067, 2019.

[126] R. D. Murphy, B. Torralva, D. P. Adams, and S. M. Yalisove, "Pump-probe imaging of laser-induced periodic surface structures after ultrafast irradiation of Si," *Appl. Phys. Lett.*, vol. 103, p. 114104, 2013.

[127] X. Jia, T. Q. Jia, N. Peng, D. H. Feng, S. A. Zhang, and Z. R. Sun, "Dynamics of femtosecond laser-induced periodic surface structures on silicon by high spatial and temporal resolution imaging," *J. Appl. Phys.*, vol. 115, p. 143102, 2014.

[128] K. Sokolowski-Tintena, A. Barty, S. Boutet, et al., "Short-pulse laser induced transient structure formation and ablation studied with time-resolved coherent XUV-scattering," *AIP Conf. Proc.*, vol. 1278 p. 373, 2010.

[129] A. Aguilar, C. Mauclair, N. Faure, J. P. Colombier, and R. Stoian, "In-situ high-resolution visualization of laser-induced periodic nanostructures driven by optical feedback," *Sci. Rep.*, vol. 7, p. 16509, 2017.

[130] A. Abou-Saleh, A. Rudenko, L. Douillard, F. Pigeon, F. Garrelie, and J. P. Colombier, "Nanoscale imaging of ultrafast light coupling to self-organized nanostructures," *ACS Photonics*, vol. 6, pp. 2287–2294, 2019.

[131] S. Khadir, D. Andrén, P. C. Chaumet, et al., "Full optical characterization of single nanoparticles using quantitative phase imaging," *Optica*, vol. 7, pp. 243–248, 2020.

[132] M. Sakakura, Y. Shimotsuma, N. Fukuda, and K. Miura, "Transient strain distributions during femtosecond laser-induced deformation inside LiF and MgO single crystals," *J. Appl. Phys.*, vol. 118, p. 023106, 2015.

[133] Y. Hayasaki, M. Isaka, A. Takita, and S. Juodkazis, "Time-resolved interferometry of femtosecond-laser induced processes under tight focusing and close-to optical breakdown inside borosilicate glass," *Opt. Express*, vol. 19, pp. 5725–5734, 2011.

[134] M. Zimmermann, A. Tausendfreund, S. Patzelt, et al., "In-process measuring procedure for sub-100 nm structures," *J. Laser Appl.* p. 24042010, 2012. https://doi.org/10.2351/1.4719936.

[135] R. Fang, A. Vorobyev, and C. Guo, "Direct visualization of the complete evolution of femtosecond laser-induced surface structural dynamics of metals," *Light Sci. Appl.*, vol. 6, p. e16256, 2017.

[136] C. Mauclair, M. Zamfirescu, G. Cheng, J. P. Colombier, E. Audouard, and R. Stoian, "Control of ultrafast laser-induced bulk nanogratings in fused silica via pulse time envelopes," *Opt. Express*, vol. 20, pp. 12997–13005, 2012.

[137] S. Höhm, A. Rosenfeld, J. Krüger, and J. Bonse, "Femtosecond diffraction dynamics of laser-induced periodic surface structures on fused silica," *Appl. Phys. Lett.*, vol. 102, p. 054102, 2013.

[138] S. Richter, A. Plech, M. Steinert, et al., "On the fundamental structure of femtosecond laser-induced nanogratings," *Laser Photonics Rev.*, vol. 6, pp. 787–792, 2012.

[139] F. Zimmermann, A. Plech, S. Richter, A. Tünnermann, and S. Nolte, "The onset of ultrashort pulse-induced nanogratings," *Laser Photonics Rev.*, vol. 10, pp. 327–334, 2016.

[140] R. Stoian, M. Wollenhaupt, T. Baumert, and I. V. Hertel, "Temporal pulse tailoring in ultrafast laser manufacturing technologies," in *Laser Precision Microfabrication*, vol. 135, K. Sugioka, M. Meunier, and A. PiquéHeidelberg, Eds, Springer-Verlag, 2010, pp. 121–144.

[141] R. Stoian, J. P. Colombier, C. Mauclair, M. K. Bhuyan, P. K. Velpula, and P. Srisungsitthisunti, "Spatial and temporal laser pulse design for material processing on ultrafast scales," *Appl. Phys. A: Mater. Process.*, vol. 114, pp. 119–127, 2014.

[142] L. Jiang, P. Liu, X. Yan, et al., "High-throughput rear-surface drilling of microchannels in glass based on electron dynamics control using femtosecond pulse trains," *Opt. Lett.*, vol. 37, pp. 781–2783, 2012.

[143] S. Hasegawa and Y. Hayasaki, "Polarization distribution control of parallel femtosecond pulses with spatial light modulators," *Opt. Express*, vol. 21, pp. 12987–12995, 2013.

[144] A. Jesacher and M. J. Booth, "Parallel direct laser writing in three dimensions with spatially dependent aberration correction," *Opt. Express*, vol. 18, pp. 21090–21099, 2010.

[145] A. Wang, L. Jiang, X. Li, et al., "Nanoscale material redistribution induced by spatially modulated femtosecond laser pulses for flexible high-efficiency surface patterning," *Opt. Express*, vol. 25, pp. 31431–31442, 2017.

[146] L. Jiang, X. S. Shi, X. Li, Y. P. Yuan, C. Wang, and Y. Lu, "Subwavelength ripples adjustment based on electron dynamics control by using shaped ultrafast laser pulse trains," *Opt. Express*, vol. 20, pp. 21505–21511, 2012.

[147] M. Forster, W. Kautek, N. Faure, E. Audouard, and R. Stoian, "Periodic nanoscale structures on polyimide surfaces generated by temporally tailored femtosecond laser pulses," *Phys. Chem. Chem. Phys*, vol. 13, pp. 4155–4158, 2011.

[148] F. Fraggelakis, E. Stratakis, and P. A. Loukakos, "Control of periodic surface structures on silicon by combined temporal and polarization shaping of femtosecond laser pulses," *Appl. Surf. Sci.*, vol. 444, pp. 154–160, 2018.

[149] F. Fraggelakis, G. Mincuzzi, J. Lopez, I. Manek-Hönninger, and R. Kling, "Controlling 2D laser nano structuring over large area with double femtosecond pulses," *Appl. Surf. Sci.*, vol. 470, pp. 677–686, 2019.

[150] H. Qiao, J. Yang, F. Wang, Y. Yang, and J. Sun, "Femtosecond laser direct writing of large-area two-dimensional metallic photonic crystal structures on tungsten surfaces," *Opt. Express*, vol. 23, p. 26617, 2015.

[151] Q. Liu, N. Zhang, J. Yang, H. Qiao, and C. Guo, "Direct fabricating large-area nanotriangle structure arrays on tungsten surface by

nonlinear lithography of two femtosecond laser beams," *Opt. Express*, vol. 26, no. 9, pp. 11718–11727, 2018.

[152] G. Meng, L. Jiang, X. Lia, et al., "Dual-scale nanoripple/ nanoparticle-covered microspikes on silicon by femtosecond double pulse train irradiation in water," *Appl. Surf. Sci.*, vol. 410, pp. 22–28, 2017.

[153] S. Höhm, M. Herzlieb, A. Rosenfeld, J. Krüger, and J. Bonse, "Dynamics of the formation of laser-induced periodic surface structures (LIPSS) upon femtosecond two-color double-pulse irradiation of metals, semiconductors, and dielectrics," *Appl. Surf. Sci.*, vol. 374, pp. 331–338, 2016.

[154] Y. Shimotsuma, M. Sakakura, P. G. Kazansky, et al., "Ultrafast manipulation of self-assembled form birefringence in glass," *Adv. Mater.*, vol. 22, pp. 4039–4043, 2010.

[155] T. Brixner, W. Pfeiffer, and F. Javier García de Abajo, "Femtosecond shaping of transverse and longitudinal light polarization," *Opt. Lett.*, vol. 29, pp. 2187–2189, 2004.

[156] M. Aeschlimann, M. Bauer, D. Bayer, et al., "Adaptive subwavelength control of nano-optical fields," *Nature*, vol. 446, pp. 301–304, 2007.

[157] P. S. Salter and M. J. Booth, "Adaptive optics in laser processing," *Light Sci. Appl.*, vol. 8, p. 110, 2019.

[158] N. Sanner, N. Huot, E. Audouard, C. Larat, J. P. Huignard, and B. Loiseaux, "Programmable focal spot shaping of amplified femtosecond laser pulses," *Opt. Lett.*, vol. 30, pp. 1479–1781, 2005.

[159] O. Martínez-Matos, P. Vaveliuk, J. G. Izquierdo, and V. Loriot, "Femtosecond spatial pulse shaping at the focal plane," *Opt. Express*, vol. 21, pp. 25010–25025, 2013.

[160] A. F. Lasagni, S. Alamri, A. I. Aguilar-Morales, F. Rößler, B. Voisiat, and T. Kunze, "Biomimetic surface structuring using laser based interferometric methods," *Appl. Sci.*, vol. 8, p. 1260, 2018.

[161] M. K. Bhuyan, P. K. Velpula, J. P. Colombier, T. Olivier, N. Faure, and R. Stoian, "Single shot high aspect ratio bulk nanostructuring of fused silica using chirp controlled ultrafast laser Bessel beams," *Appl. Phys. Lett.*, vol. 104, p. 021107, 2014.

[162] J. Hamazaki, R. Morita, K. Chujo, K. Kobayashi, S. Tanda, and T. Omatsu, "Optical-vortex laser ablation," *Opt. Express*, vol. 18, pp. 2144–2151, 2010.

[163] J. J. Nivas, F. Cardano, Z. Song, et al., "Surface structuring with polarization-singular femtosecond laser beams generated by a q-plate," *Sci. Rep.*, vol. 7, p. 42142, 2017.

[164] C. Hnatovsky, V. Shvedov, W. Krolikowski, and A. Rode, "Revealing local field structure of focused ultrashort pulses," *Phys. Rev. Lett.*, vol. 106, p. 123901, 2011.

[165] H. Zhang, C. Li, E. Bevillon, J. P. Colombier, G. Cheng, and R. Stoian, "Ultrafast destructuring of laser-irradiated tungsten: thermal or nonthermal process," *Phys. Rev. B*, vol. 94, p. 224103, 2016.

[166] K. König and A. Ostendorf, Eds., *Optically Induced Nanostructures: Biomedical and Technical Applications*, Berlin, De Gruyter, 2015.

[167] V. P. Veiko and V. I. Konov, Eds., *Fundamentals of Laser-assisted Micro- and Nanotechnologies*, *Springer Series in Materials Science*, Springer, 2014.

[168] N. A. Vainos, Ed. *Laser Growth and Processing of Photonic Devices*, *Woodhead Publishing Series in Electronic and Optical Materials*, Woodhead Publishing, 2012.

[169] J. Bonse, S. Höhm, S. V. Kirner, A. Rosenfeld, and J. Krüger, "Laser-induced periodic surface structures – a scientific evergreen," *IEEE J. Sel. Top. Quant. Electron.*, vol. 23, p. 9000615, 2017.

[170] K. Sugioka and Y. Cheng, Eds., Laser-based nano fabrication and nano lithography, Nanomaterials, MDPI, 2020, https://doi.org/10.3390/books978-3-03897-411-6.

[171] F. A. Müller, C. Kunz, and S. Gräf, "Bio-inspired functional surfaces based on laser-induced periodic surface structures," *Materials*, vol. 9, p. 476, 2016.

[172] A. Y. Vorobyev and C. Guo, "Colorizing metals with femtosecond laser pulses," *Appl. Phys. Lett.*, vol. 92, p. 041914, 2008.

[173] B. Dusser, Z. Sagan, H. Soder, et al., "Controlled nanostructrures formation by ultra fast laser pulses for color marking," *Opt. Express*, vol. 18, pp. 2913–2924, 2010.

[174] G. Zhang, G. Cheng, M. K. Bhuyan, C. D'Amico, W. Zhao, and R. Stoian, "Ultrafast Bessel laser beam writing of Bragg gratings waveguide and its application as temperature sensor," *Photonics Res.*, vol. 7, pp. 806–814, 2019.

[175] J. Zhang, M. Gecevičius, M. Beresna, and P. G. Kazansky, "Seemingly unlimited lifetime data storage in nanostructured glass," *Phys. Rev. Lett.*, vol. 112, p. 033901, 2014.

[176] B. McMillen, C. Athanasiou, and Y. Bellouard, "Femtosecond laser direct-write waveplates based on stress-induced birefringence," *Opt. Express*, vol. 24, pp. 27239–27252, 2016.

[177] L. Jiao, Z. Y. Chua, S. K. Moon, J. Song, G. Bi, and H. Zheng, "Femtosecond laser produced hydrophobic hierarchical structures on additive manufacturing parts," *Nanomaterials*, vol. 8, p. 601, 2018.

[178] E. P. Ivanova, J. Hasan, H. K. Webb, et al., "Bactericidal activity of black silicon," *Nat. Commun.*, vol. 4, p. 2838, 2013.

[179] J. M. Guay, A. Cala Lesina, G. Cote, et al., "Laser-induced plasmonic colours on metals," *Nat. Commun.*, vol. 8, p. 16095, 2017.

[180] M. Martínez-Calderon, J. J. Azkona, N. Casquero, et al., "Tailoring diamond's optical properties via direct femtosecond laser nanostructuring," *Sci. Rep.*, vol. 8, p. 14262, 2018.

[181] K. C. Park, H. J. Choi, C. H. Chang, R. E. Cohen, G. H. McKinley, and G. Barbastathis, "Nanotextured silica surfaces with robust superhydrophobicity and omnidirectional broadband supertransmissivity," *ACS Nano*, vol. 6, pp. 3789–3799, 2012.

[182] A. J. Pedraza, J. D. Fowlkes, and D. H. Lowndes, "Silicon microcolumn arrays grown by nanosecond pulsed-excimer laser irradiation," *Appl. Phys. Lett.*, vol. 74, pp. 2322–2324, 1999.

[183] C. Wu, C. H. Crouch, L. Zhao, et al., "Near-unity below-band-gap absorption by microstructured silicon," *Appl. Phys. Lett.*, vol. 78, p. 1850, 2001.

[184] M. Aeschlimann, T. Brixner, D. Differt, et al., "Perfect absorption in nanotextured thin films via Anderson-localized photon modes," *Nat. Photonics*, vol. 9, pp. 663–668, 2015.

[185] M. Ams, P. Dekker, S. Gross, and M. J. Withford, "Fabricating waveguide Bragg gratings (WBGs) in bulk materials using ultrashort laser pulses," *Nanophotonics*, vol. 6, pp. 743–763, 2017.

[186] N. Sharma, N. Destouches, C. Florian, R. Serna, and J. Siegel, "Tailoring metal-dielectric nanocomposite materials with ultrashort laser pulses for dichroic color control," *Nanoscale*, vol. 11, pp. 18779–18789, 2019.

[187] L. Canioni, M. Bellec, A. Royon, B. Bousquet, and T. Cardinal, "Three-dimensional optical data storage using third-harmonic generation in silver zinc phosphate glass," *Opt. Lett.*, vol. 33, pp. 360–362, 2008.

[188] R. N. Wenzel, "Resistance of solid surfaces to wetting by water," *Chem. Res.*, vol. 28, pp. 988–994, 1936.

[189] A. B. D. Cassie and S. Baxter, "Wettability of porous surfaces," *Trans. Faraday Soc.*, vol. 40, pp. 546–551, 1944.

[190] C. Florian, J. L. Déziel, S. V. Kirner, J. Siegel, and J. Bonse, "The role of the laser-induced oxide layer in the formation of laser-induced periodic surface structures," *Nanomaterials*, vol. 10, p. 147, 2020.

[191] C. Frischkorn and M. Wolf, "Femtochemistry at metal surfaces: nonadiabatic reaction dynamics," *Chem. Rev.*, vol. 106, pp. 4207–423, 2006.

[192] Y. Lin, J. Han, M. Cai, et al., "Durable and robust transparent superhydrophobic glass surfaces fabricated by a femtosecond laser with exceptional water repellency and thermostability," *J. Mater. Chem.*, vol. 6, pp. 9049–9056, 2018.

[193] V. Kohli, V. Robles, M. L. Cancela, J. P. Acker, A. J. Waskiewicz, and A. Y. Elezzabi, "An alternative method for delivering exogenous material into developing zebrafish embryos," *Biotechnol. Bioeng.*, vol. 98, pp. 1230–1241, 2007.

[194] M. Pospiech, M. Emons, K. Kuetemeyer, A. Heisterkamp, and U. Morgner, "Superresolved femtosecond laser nanosurgery of cells," *Biomed. Opt. Express*, vol. 2, pp. 264–271, 2011.

[195] M. Martínez-Calderon, M. Manso-Silván, A. Rodríguez, et al., "Surface micro- and nano-texturing of stainless steel by femtosecond laser for the control of cell migration," *Sci. Rep.*, vol. 6, p. 36296, 2016.

[196] U. K. Tirlapur and K. Kïg, "Targeted transfection by femtosecond laser," *Nature*, vol. 418, pp. 290–291, 2002.

[197] M. Antkowiak, M. Torres-Mapa, D. Stevenson, K. Dholakia, and F. J. Gunn-Moore, "Femtosecond optical transfection of individual mammalian cells," *Nat. Protoc.*, vol. 8, pp. 1216–1233, 2013.